A LAVRENTIEV PHENOMENON IN THE NEO-HOOKEAN MODEL

MARCO BARCHIESI, DUVAN HENAO, CARLOS MORA-CORRAL, AND RÉMY RODIAC

Abstract. We exhibit a Lavrentiev gap phenomenon for the neo-Hookean energy in three-dimensional nonlinear elasticity. More precisely, we construct boundary data for which the infimum of the neo-Hookean energy over deformations satisfying a natural regularity and invertibility condition is strictly larger than the infimum over the weak H^1-closure of that class. The mechanism underlying the gap is a deformation with a dipole-type singularity.

1. Introduction

1.1. **Overview of the problem and statement of the result.** The neo-Hookean model is one of the simplest models in nonlinear elasticity. In this model, a deformation $\boldsymbol{u} : \Omega \to \mathbb{R}^3$ of an elastic body in a reference configuration $\Omega \subset \mathbb{R}^3$ is assumed to minimise an energy of the form

$$E(\boldsymbol{u}) = \int_\Omega \left[|D\boldsymbol{u}|^2 + H(|\det D\boldsymbol{u}|) \right] \mathrm{d}\boldsymbol{x}, \tag{1.1}$$

where $H : (0,\infty) \to [0,\infty)$ is a suitable convex function such that

$$\lim_{t\to\infty} \frac{H(t)}{t} = \lim_{s\to 0} H(s) = \infty. \tag{1.2}$$

The main mathematical difficulty is to identify an admissible class for which the minimisation of E is both physically meaningful and analytically tractable. Physical admissibility requires the deformation to preserve orientation and exclude interpenetration of matter, so two natural mathematical restrictions for the deformation are that $\boldsymbol{u}$ is one-to-one almost everywhere (a.e.), and $\det D\boldsymbol{u} > 0$ a.e. As a boundary condition, we prescribe a bi-Lipschitz orientation-preserving map $\boldsymbol{b} : \Omega \to \mathbb{R}^3$. In fact, for technical convenience, we impose the Dirichlet condition in a strong form: we fix a smooth bounded domain $\widetilde{\Omega}$ compactly contained in Ω and require that each admissible deformation agrees with $\boldsymbol{b}$ on the entire complement $\Omega \setminus \widetilde{\Omega}$, not merely on $\partial\Omega$. This leads naturally to the admissible class

$$\mathcal{A} = \mathcal{A}(\Omega, \widetilde{\Omega}, \boldsymbol{b}) := \{\boldsymbol{u} \in H^1(\Omega,\mathbb{R}^3) \colon \boldsymbol{u} = \boldsymbol{b} \text{ in } \Omega \setminus \widetilde{\Omega},\ \boldsymbol{u} \text{ is one-to-one a.e.,} \\ \det D\boldsymbol{u} > 0 \text{ a.e., and } E(\boldsymbol{u}) < \infty\}.$$

However, due to the possibility of cavitation, i.e., the formation of voids in the material, it was shown in [5] that E is not lower semicontinuous in $\mathcal{A}$. Since the difficulty is the possible appearance of many cavities, one can try to add a term to penalize the formation of cavities in the energy (1.1), or to add a condition in the minimisation space to exclude cavitation. This is the approach followed by Müller and Spector [30], where they also introduced the nowadays well-known condition INV in order to rule out some pathological examples of cavitation. Condition INV, which is a stronger form of invertibility than the property of being one-to-one a.e., informally means that after the deformation, matter coming from any subregion U remains enclosed by the image of ∂U and matter coming from outside U remains exterior to the region enclosed by the image of ∂U. An alternative approach was devised in [25, 26] where, instead of condition INV, the authors work with one-to-one a.e. maps but penalize the formation of cavities by using the "divergence identities". These are a generalisation of the identity $\operatorname{Det} D\boldsymbol{u} = \det D\boldsymbol{u}$, which

Date: November 4, 2026.

holds in absence of cavitation, where $\operatorname{Det} D\boldsymbol{u} := \frac{1}{3}\operatorname{div}(\operatorname{cof} D\boldsymbol{u}^T\boldsymbol{u})$ denotes the distributional Jacobian. Both approaches are successful in treating energies slightly more coercive than (1.1), for example energies like (1.1) where $|D\boldsymbol{u}|^2$ is replaced by $|D\boldsymbol{u}|^p$ for some $p > 2$, but fail to provide minimisers for (1.1). The difficulty is that, although condition INV and the divergence identities are well defined in the limiting case $p = 2$ (see [13, 27]), they are not sequentially closed with respect to the weak H^1 convergence. This was demonstrated by an example of Conti and De Lellis [13, Theorem 6.1], see also [8, 14, 10]. This lack of compactness prevents the application of the direct method of the calculus of variations. *The goal of this paper* is to show that this lack of compactness is also related to a *Lavrentiev phenomenon*. More precisely, we investigate the minimisation of (1.1) in the space

$$\mathcal{A}^r = \mathcal{A}^r(\Omega, \widetilde{\Omega}, \boldsymbol{b}) := \{\boldsymbol{u} \in \mathcal{A} \colon \Omega_{\boldsymbol{b}} = \operatorname{im}_{\mathrm{G}}(\boldsymbol{u}, \Omega) \text{ a.e. and } \boldsymbol{u}^{-1} \in W^{1,1}(\Omega_{\boldsymbol{b}}, \mathbb{R}^3)\}, \tag{1.3}$$

where $\Omega_{\boldsymbol{b}} := \boldsymbol{b}(\Omega)$ and $\operatorname{im}_{\mathrm{G}}(\boldsymbol{u}, \Omega)$ is the geometric image defined in Definition 2.2. Here, the superscript r stands for *regular*. Indeed, by using [9, Lemma 2.10] and [6, Lemma 5.1], one can show that maps in $\mathcal{A}^r$ are regular in the sense that they satisfy condition INV and the divergence identities (and, hence, they do not open any cavity). Our main result is the following.

Theorem 1.1. *Let $\Omega = B(\mathbf{0}, 4)$, and assume that H is convex and satisfies* (1.2) *and*

$$H(t) \le c\, t^{-\alpha} \quad \text{as } t \to 0^+ \qquad \text{and} \qquad H(t) \le c\, t^{\beta} \quad \text{as } t \to \infty, \tag{1.4}$$

for some $\alpha < \frac{1}{3}$, $\beta < \frac{3}{2}$, and $c > 0$. Then, there exist a subdomain $\widetilde{\Omega} \subset\subset \Omega$ and a bi-Lipschitz homeomorphism $\boldsymbol{b} : \Omega \to \mathbb{R}^3$ such that

$$\inf\{E(\boldsymbol{u}) \colon \boldsymbol{u} \in \mathcal{A}^r\} > \inf\{E(\boldsymbol{u}) \colon \boldsymbol{u} \in \overline{\mathcal{A}^r}\}, \tag{1.5}$$

where $\overline{\mathcal{A}^r}$ is the closure of $\mathcal{A}^r$ with respect to the weak convergence in H^1.

The additional upper growth bounds (1.4) are sufficient conditions for the construction used in the proof of the theorem. The restrictions $\alpha < 1/3$ and $\beta < 3/2$ come from the integrability estimates for the term $H(\det D\mathbf{u})$; see Appendix for the detailed calculations. These upper growth bounds are compatible with (1.2).

Several remarks are in order concerning this theorem. First, it is not known if the infimum on the right-hand side of (1.5) is attained. This is because we do not know if $\det D\boldsymbol{u}_n \rightharpoonup \det D\boldsymbol{u}$ weakly in L^1 whenever $(\boldsymbol{u}_n)_n \subset \mathcal{A}^r$ is a minimising sequence for E. Nevertheless, with the same proof used for Theorem 1.1 we can provide slightly different Lavrentiev phenomena where the infimum in $\overline{\mathcal{A}^r}$ is attained; see Section 4. Indeed, it was shown in [28, Theorem 4.3] (see also [15] for earlier existence results) that the infimum of E in the sequential weak closure in H^1 of homeomorphisms in H^1 satisfying $\det D\boldsymbol{u} \ge 0$ a.e., Lusin's condition (N) and agreeing with $\boldsymbol{b}$ on $\Omega \setminus \widetilde{\Omega}$ is attained. However, a slight modification of Theorem 1.1 (see Theorem 4.2) shows that, under assumption (1.4), the minimisers obtained in [28] must have some singularity. Hence, the classical strategy of the calculus of variations, which consists of finding a minimiser of the energy in a larger space and then showing that minimisers are more regular, cannot work in the presence of a Lavrentiev phenomenon. This is an argument for using a relaxed energy instead of the original energy E; this strategy was developed in [7, 8, 9].

Second, we notice that if the convex function H in (1.1) satisfies (1.2) and if there exists $c > 0$ such that

$$c^{-1}H(t) \le H(2t) \le c\, H(t), \quad H(t) \ge \frac{1}{t^2}, \text{ for all } t \in (0, \infty), \tag{1.6}$$

then a weak H^1 limit of orientation preserving homeomorphisms in $\mathcal{A}$ does satisfy condition INV; see [14]. This suggests that, under the growth condition (1.6) there is no Lavrentiev gap phenomenon for E as the one in Theorem 1.1.

Third, it was recently shown in [11] that even less coercive energies than (1.1) admit minimisers in the sequential weak closure of some Sobolev, orientation preserving homeomorphisms. These

energies are of the form $E(\boldsymbol{u}) = \int_\Omega [|D\boldsymbol{u}|^p + H(\det D\boldsymbol{u})]$ with $1 < p < 2$. It would be interesting to know if a Lavrentiev gap phenomenon holds in that case.

Fourth, we observe that there is a strong analogy between the problem of minimising the neo-Hookean energy among regular maps and the problem of minimising the Dirichlet energy for maps $\boldsymbol{u} : \Omega \subset \mathbb{R}^3 \to \mathbb{S}^2$ among continuous maps. This analogy was already observed in [21, 22] and shows that the lack of compactness of both problems is caused by maps with dipole-like singularities. From that point of view, our Theorem 1.1 can be seen as an analogue of [23, Theorem B]. We also refer to [24] and [29] for more on the Lavrentiev gap phenomenon for harmonic maps, in particular we can ask if Lavrentiev gap phenomena such as the one in Theorem 1.1 hold for many boundary data, since it is the case in the context of harmonic maps, as shown in [29]. In the next section we present several Lavrentiev gap phenomena discovered in nonlinear elasticity.

1.2. **Lavrentiev gap phenomena in elasticity.** In nonlinear elasticity, the Lavrentiev phenomenon was first observed by Ball [2] for genuinely cavitating deformations, i.e., with cavities that actually open a hole. This is not the mechanism underlying Theorem 1.1, in which a cavity is formed and then filled from material coming from another cavity, so that $\Omega_{\boldsymbol{b}} = \mathrm{im}_{\mathrm{G}}(\boldsymbol{u}, \Omega)$ a.e. From the analytical point of view, this is reflected in the fact that a true cavitation map cannot be approximated within $\mathcal{A}^r$ under a uniform bound on the neo-Hookean energy, because such a bound would force the Jacobians to be equi-integrable. By contrast, the dipole singularity relevant here does admit an approximation by maps in $\mathcal{A}^r$ with equibounded neo-Hookean energy.

The question whether the Lavrentiev phenomenon can occur under growth conditions on the stored-energy density that imply continuity of all finite-energy deformations was raised by Ball and Mizel [4] (see also Ball [3]). This question was answered affirmatively in two dimensions by Foss [18] and Foss, Hrusa and Mizel [19, 20], who constructed examples on a disk sector with a smooth, polyconvex, frame-indifferent energy density W satisfying $W(F) \geq c\,|F|^p - C$ for some $p > 2$ and $W(F) \to \infty$ as $\det F \to 0^+$. In those examples, the Lavrentiev gap is driven by the local behaviour of almost minimisers near the tip of the sector, interacting with prescribed boundary conditions.

More recently, Almi, Krömer and Molchanova [1] produced Lavrentiev gaps in dimensions $d = 2$ and $d = 3$ for a neo-Hookean-type density $W(F) = |F|^p + \gamma(\det F)^{-q}$ with $p > d$, $1 < q < p/(p-2)$, and $\gamma = pd^{\frac{p}{2}-1}/q$. Their admissible class consists of orientation-preserving $W^{1,p}$-maps satisfying the Ciarlet–Nečas condition [12], which (in the regime $p > d$, hence for continuous maps) implies almost everywhere injectivity. The gap in [1] separates $W^{1,p}$-deformations from $W^{1,\infty}$-deformations. It is generated by a global self-contact mechanism: for a suitable choice of boundary conditions on a disconnected domain, one can compress two cross-sections onto the same point (or line), creating self-contact while keeping the energy arbitrarily small; by contrast, Lipschitz competitors satisfying the Ciarlet–Nečas condition are necessarily injective everywhere (as a consequence of Reshetnyak's theorem for mappings of finite distortion) and must therefore "go around" the obstruction, incurring a strictly positive energy cost.

The present paper exhibits a Lavrentiev phenomenon of a fundamentally different nature, distinguished from the existing literature in two complementary respects:

(i) Natural coercivity exponent and physical energy. We work in three dimensions with the standard neo-Hookean functional

$$E(\boldsymbol{u}) = \int_\Omega \left[|D\boldsymbol{u}|^2 + H(|\det D\boldsymbol{u}|)\right] \,\mathrm{d}\boldsymbol{x}.$$

The coercivity exponent here is $p = 2 < d = 3$, namely the physically natural regime in which Sobolev embedding does not yield continuity of finite-energy deformations. By contrast, the examples in [1, 18, 19, 20] are constructed in the continuity regime $p > d$.

(ii) Gap driven by inverse regularity and lack of weak closure. In our setting, the energy gap does not arise from comparing two regularity levels of the forward deformation $\boldsymbol{u}$ within a fixed notion of injectivity. Rather, it stems from the failure of the physically motivated class $\mathcal{A}^r$ to be sequentially closed under weak H^1-convergence. Accordingly, the gap separates $\mathcal{A}^r$ from its weak closure $\overline{\mathcal{A}^r}$ and is governed by the regularity of the *inverse* deformation (Sobolev versus BV), rather than an additional regularity of $\boldsymbol{u}$ itself.

This should be contrasted with [1]. There, the admissibility condition is stable under weak convergence, but the class remains broad enough to permit low-energy deep self-contact. Here, by contrast, the admissible class rules out interpenetration but loses weak compactness. Thus [1] points to an admissible class that is too large, whereas our example points to one that is too small.

1.3. **Strategy of the proof and organisation of the paper.** The proof of Theorem 1.1 is based on results that appeared in the series of papers [7, 8, 9] and on the use of the Conti–De Lellis dipole map and its regularised sequence. More precisely, we have shown in [7, 8, 9] that any sequence of regular maps approximating the Conti–De Lellis map produces a jump of energy of at least 2π in the limit. By using this observation and by constructing a suitable interpolation between the Conti–De Lellis map and a regularised sequence we can construct a boundary data for which we obtain the desired gap phenomenon.

The paper is organised as follows. Section 2 recalls some results from [7, 8, 9] and the basic properties of the Conti–De Lellis map. These ingredients are used in Section 3 to prove our main result, Theorem 1.1. Section 4 presents two variants in which the infimum over the larger class is attained. The main technical ingredient in the proof of Theorem 1.1 is the construction of a boundary data obtained from the Conti–De Lellis map and its regularised sequence. That construction is deferred to Appendix C, after Appendices A and B where the precise definitions of the Conti–De Lellis map and its regularised sequences are given.

2. The relaxed energy and the Conti–De Lellis map

2.1. **The relaxed energy.** In [7, 8, 9] the authors have proposed an approach to the minimisation problem for E based on relaxation, by providing a larger space $\mathcal{B} \supset \mathcal{A}^r$ that is *compact* for sequences with equibounded energy. In order to define this space we first define the *geometric image* of a map $\boldsymbol{u} \in \mathcal{A}$. We recall that maps in $H^1(\Omega, \mathbb{R}^3)$ are approximately differentiable a.e.; see, e.g., [16, Theorem 6.4]. We denote the approximate gradient by $\nabla \boldsymbol{u}$ and the distributional derivative by $D\boldsymbol{u}$.

Definition 2.1. Let $\boldsymbol{u}$ be approximately differentiable a.e. and such that $\det D\boldsymbol{u} \neq 0$ a.e. We define Ω_0 as the set of $\boldsymbol{x} \in \Omega$ for which the following are satisfied:

(1) the approximate differential of $\boldsymbol{u}$ at $\boldsymbol{x}$ exists and equals $D\boldsymbol{u}(\boldsymbol{x})$,
(2) there exist $\boldsymbol{w} \in C^1(\mathbb{R}^3, \mathbb{R}^3)$ and a compact set $K \subset \Omega$ of density 1 at $\boldsymbol{x}$ such that $\boldsymbol{u}|_K = \boldsymbol{w}|_K$ and $\nabla \boldsymbol{u}|_K = D\boldsymbol{w}|_K$,
(3) $\det \nabla \boldsymbol{u}(\boldsymbol{x}) \neq 0$.

From [17, Theorem 3.1.8], Rademacher's Theorem and Whitney's Theorem we infer that Ω_0 is a set of full Lebesgue measure in Ω, i.e., $|\Omega \setminus \Omega_0| = 0$.

Definition 2.2. For any measurable set A of Ω, the geometric image of A under an a.e. approximately differentiable map $\boldsymbol{u}$ is defined by

$$\mathrm{im}_{\mathrm{G}}(\boldsymbol{u}, A) := \boldsymbol{u}(A \cap \Omega_0),$$

with Ω_0 as in Definition 2.1.

The notion of geometric image is used in the definition of the space

$$\mathcal{B} := \{\boldsymbol{u} \in H^1(\Omega,\mathbb{R}^3)\colon \boldsymbol{u} = \boldsymbol{b} \text{ in } \Omega \setminus \widetilde{\Omega},\ \boldsymbol{u} \text{ is one-to-one a.e., } \det D\boldsymbol{u} \neq 0 \text{ a.e.,}$$
$$\Omega_{\boldsymbol{b}} = \mathrm{im}_{\mathrm{G}}(\boldsymbol{u},\Omega) \text{ a.e., } \boldsymbol{u}^{-1} \in BV(\Omega_{\boldsymbol{b}},\mathbb{R}^3), \text{ and } E(\boldsymbol{u}) < \infty\}.$$

On this set $\mathcal{B}$ it is possible to define a *lower semicontinuous* energy F extending E, namely

$$F(\boldsymbol{u}) := E(\boldsymbol{u}) + 2\|D^s\boldsymbol{u}^{-1}\| \text{ for } \boldsymbol{u} \in \mathcal{B}.$$

Here $D^s\boldsymbol{u}^{-1}$ is the singular part of the distributional gradient of the inverse (which is a matrix-valued Radon measure), and $\|D^s\boldsymbol{u}^{-1}\|$ is its norm. Then, by using the direct method of the calculus of variations, one can obtain that the energy F admits a minimiser $\boldsymbol{u}$ on $\mathcal{B}$. In this way the existence problem of a minimiser for E is reduced to showing that $\boldsymbol{u}$ belongs to $\mathcal{A}^r$. This is summarised in the following result.

Theorem 2.1. [9, Theorem 1.1] *Let $\{\boldsymbol{u}_j\}_j$ be a sequence in $\mathcal{B}$ such that $\{F(\boldsymbol{u}_j)\}_j$ is equibounded. Then there exists $\boldsymbol{u} \in \mathcal{B}$ such that, up to a subsequence, $\boldsymbol{u}_j \rightharpoonup \boldsymbol{u}$ in $H^1(\Omega,\mathbb{R}^3)$ and*

$$\liminf_{j\to\infty} F(\boldsymbol{u}_j) \geq F(\boldsymbol{u}).$$

In particular, the energy F has a minimiser in $\mathcal{B}$.

2.2. **The Conti–De Lellis map.** Since the singular map $\boldsymbol{v}$ of Conti–De Lellis plays a central role in our construction, we briefly describe it and provide pictures here; for the details we refer the reader to Appendix A. The Conti–De Lellis map is an axisymmetric map defined in $B(\mathbf{0},4)$ with boundary condition equal to the identity. We remark that $\boldsymbol{v} \in \mathcal{B}$ and $\det D\boldsymbol{v} > 0$ a.e., but $\boldsymbol{v} \notin \mathcal{A}^r$. Indeed, the third component of the inverse is not Sobolev, but it belongs to the class SBV (special functions of bounded variation). The key feature of $\boldsymbol{v}$ is that it brings into contact two portions of the body that were initially at unit distance apart, namely, the half-balls

$$a := \{\boldsymbol{x} :\ x_1^2 + x_2^2 + x_3^2 < 1,\ x_3 < 0\} \quad \text{and} \quad e := \{\boldsymbol{x} :\ x_1^2 + x_2^2 + (x_3-1)^2 < 1,\ x_3 > 1\}$$

(see Figure 1) are put in contact with each other across the "bubble"

$$\Gamma := \{(y_1,y_2,y_3) :\ y_1^2 + y_2^2 + (y_3 - \tfrac{1}{2})^2 = (\tfrac{1}{2})^2\},$$

which in turn comes entirely from only two singular points: the origin $\mathbf{0}$ and $\mathbf{0}' = (0,0,1)$. At $\mathbf{0}'$ a cavity is nucleated and subsequently filled by material originating from the half-ball a, which passes through the origin. We refer to this structure as a *dipole*. The jump set of the third component of the inverse coincides with the sphere Γ, and the amplitude of the jump is given by the distance between the poles $\mathbf{0}$ and $\mathbf{0}'$. Consequently $F(\boldsymbol{v}) = E(\boldsymbol{v}) + 2\pi$.

It was shown in [8, Theorem 1.2] that the dipole map $\boldsymbol{v}$ can be approximated by a sequence of maps $\boldsymbol{u}_\varepsilon \in \mathcal{A}^r$ from the energy point of view, i.e., $\boldsymbol{u}_\varepsilon \rightharpoonup \boldsymbol{v}$ in H^1 and $\lim_{\varepsilon\to 0} E(\boldsymbol{u}_\varepsilon) = F(\boldsymbol{v})$. Roughly speaking, the maps $\boldsymbol{u}_\varepsilon$ are obtained from $\boldsymbol{v}$ by regularizing the jump of the inverse through a smooth junction (see the red layer in Figure 2). For the details we refer the reader to Appendix B.

The rough idea of the proof of Theorem 1.1 is to use $\boldsymbol{v}$ as a boundary data to force approximate minimisers of the energy E to have the same singularities as $\boldsymbol{v}$. However, the map $\boldsymbol{v}$ is not one-to-one: the segment $S := \{(0,0,x_3)\colon x_3 \in (0,1)\}$, the punctured disks $D := \{(x_1,x_2,0)\colon 0 < x_1^2 + x_2^2 \leq 1\}$ and $D' := \{(x_1,x_2,1)\colon 0 < x_1^2 + x_2^2 \leq 1\}$, and the semisphere $\{\boldsymbol{x} :\ x_1^2 + x_2^2 + x_3^2 = 1,\ x_3 < 0\}$ are contracted onto the origin. Nevertheless, outside the region

$$U := \{\boldsymbol{x} :\ x_1^2 + x_2^2 + x_3^2 \leq 1,\ x_3 \leq 0\} \cup S \cup D' \tag{2.1}$$

it is regular and it can be "patched". This means that we can construct a bi-Lipschitz homeomorphism from $B(\mathbf{0},4)$ that agrees with $\boldsymbol{v}$ outside a small neighbourhood of U. This construction is the main ingredient in the proof of Theorem 1.1.

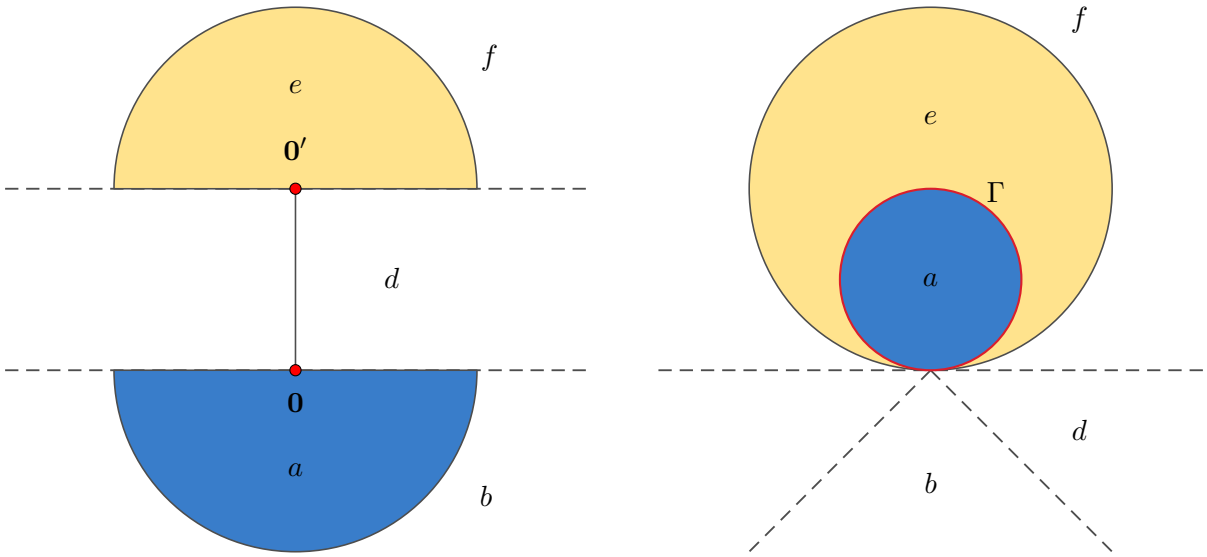


FIGURE 1. Reference (left) and deformed (right) configurations ($2D$ sections) of the map $\boldsymbol{v}$ by Conti and De Lellis

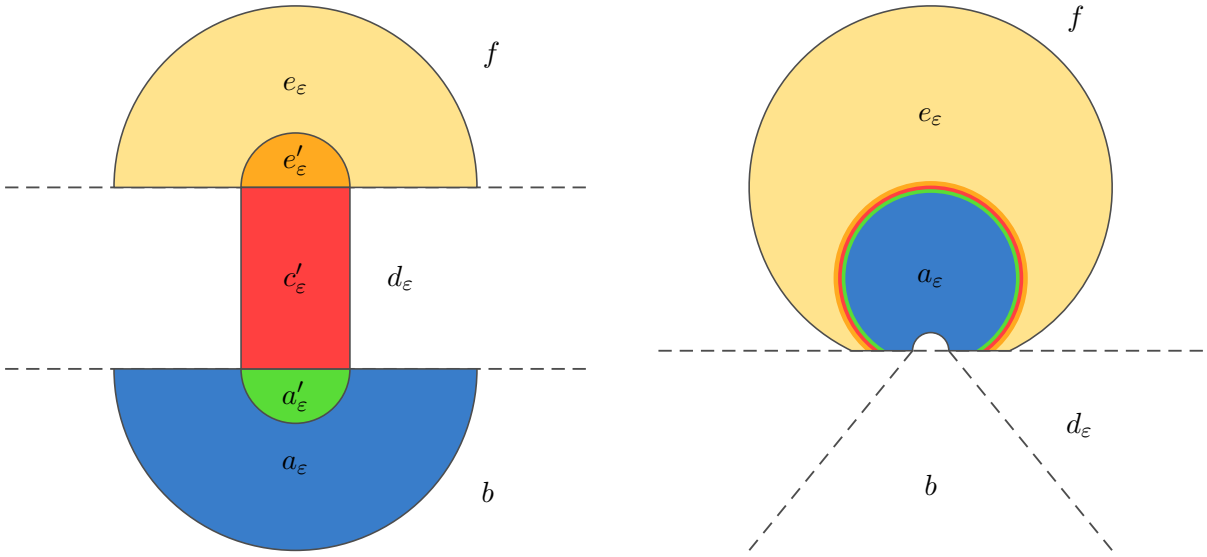


FIGURE 2. Reference (left) and deformed (right) configurations ($2D$ sections) of the approximating map $\boldsymbol{u}_\varepsilon$

3. Proof of Theorem 1.1

We now proceed to the proof of Theorem 1.1 and start by a result containing the patching process alluded to in the previous section, where $\boldsymbol{v}$ is modified in the neighbourhood

$$U_\delta := \{\boldsymbol{x} \in B(\mathbf{0}, 4) \colon \operatorname{dist}(\boldsymbol{x}, U) < \delta\}, \qquad \delta \in (0, 1]$$

of U (see Figure 3, in blue).

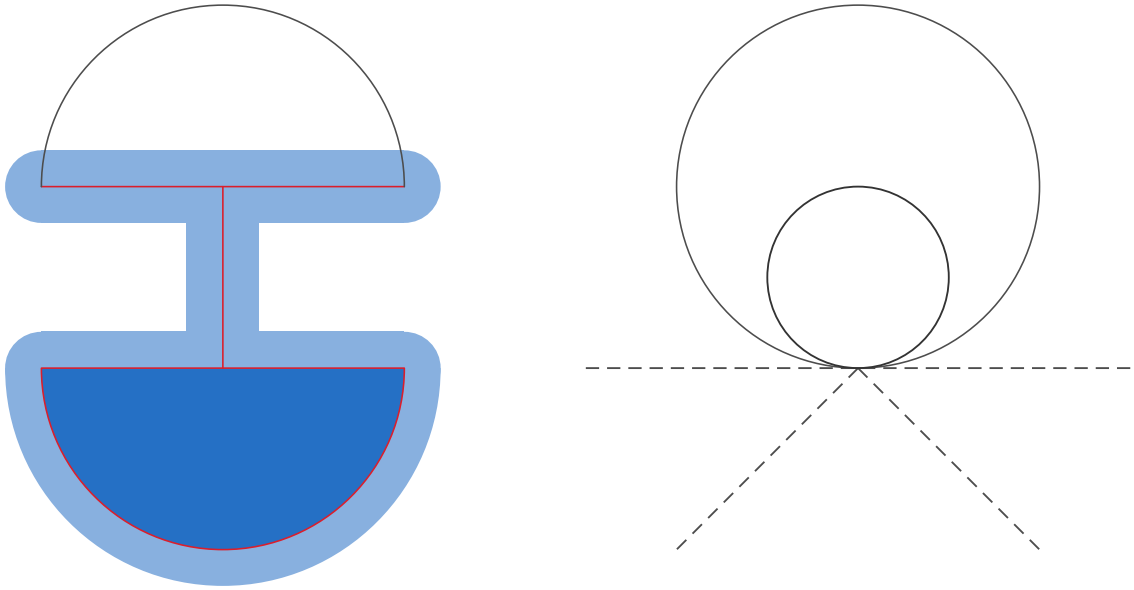


FIGURE 3. In blue the $2D$ section of the region U_δ

Theorem 3.1. *For each $\delta \in (0,1]$ there exists a bi-Lipschitz orientation-preserving homeomorphism $\boldsymbol{b}_\delta : B(\mathbf{0},4) \to \mathbb{R}^3$ such that $\boldsymbol{b}_\delta = \boldsymbol{v}$ on $B(\mathbf{0},4)\setminus U_\delta$. Moreover, if H is convex and satisfies* (1.2) *and* (1.4) *for some $\alpha < \frac{1}{3}$, $\beta < \frac{3}{2}$, and $c > 0$, then $\{E(\boldsymbol{b}_\delta)\}_{\delta>0}$ is equibounded.*

Because the proof is technical, we defer it to Appendix C.

In what follows, when $\Omega = B(\mathbf{0},4)$, $\widetilde{\Omega} = U_\delta$ and $\boldsymbol{b} = \boldsymbol{b}_\delta$, we rename the family $\mathcal{A}^r = \mathcal{A}^r(\Omega, \widetilde{\Omega}, \boldsymbol{b})$ as $\mathcal{A}^r_\delta$, where $\boldsymbol{b}_\delta$ is as in Theorem 3.1. Moreover, let $\overline{\mathcal{A}^r_\delta}$ denote the weak sequential closure of $\mathcal{A}^r_\delta$ in H^1. Because of the construction of the $\boldsymbol{b}_\delta$ in Theorem 3.1, we have that

$$\mathcal{A}^r_{\delta'} \subset \mathcal{A}^r_\delta \qquad \text{for } 0 < \delta' \le \delta \le 1. \tag{3.1}$$

In our example, $\mathcal{A}^r_\delta$ plays the role of the regular class and the underlying mechanism of the Lavrentiev phenomenon is the energy concentration of the dipole $\boldsymbol{v}$ at the two singular points, $\mathbf{0}$ and $\mathbf{0}'$. This amount of energy is precisely $2\pi = 2\|D^s \boldsymbol{v}^{-1}\|$ and cannot be detected by E.

We present the main result of the article, of which Theorem 1.1 is a particular case.

Theorem 3.2. *Assume that H is a convex function that satisfies conditions* (1.2) *and* (1.4). *Then, for all $\lambda \in (0, 2\pi)$ there exists $\delta \in (0,1]$ such that*

$$\inf\{E(\boldsymbol{u})\colon \boldsymbol{u} \in \mathcal{A}^r_\delta\} \ge \inf\{E(\boldsymbol{u})\colon \boldsymbol{u} \in \overline{\mathcal{A}^r_\delta}\} + \lambda.$$

Proof. Suppose, for the sake of contradiction, that the claim is false for some $\lambda \in (0, 2\pi)$. Then, for any $\delta \in (0,1]$ we can select $\boldsymbol{w}_\delta \in \mathcal{A}^r_\delta$ such that

$$E(\boldsymbol{w}_\delta) < \inf\{E(\boldsymbol{u})\colon \boldsymbol{u} \in \overline{\mathcal{A}^r_\delta}\} + \lambda. \tag{3.2}$$

As $\boldsymbol{b}_\delta \in \mathcal{A}^r_\delta$, we can choose $\boldsymbol{w}_\delta$ such that $E(\boldsymbol{w}_\delta) \le E(\boldsymbol{b}_\delta)$. Then, by Theorem 3.1, the set $\{E(\boldsymbol{w}_\delta)\}_{\delta\in(0,1]}$ is bounded. From (3.1) we obtain that $\boldsymbol{w}_\delta \in \mathcal{A}^r_1$. Then, by Theorem 2.1, there exist a sequence $\{\delta_j\}_j$ in $(0,1]$ tending to zero and a map $\boldsymbol{w} \in \overline{\mathcal{A}^r_1}$ such that

$$\boldsymbol{w}_{\delta_j} \rightharpoonup \boldsymbol{w} \text{ in } H^1(\Omega,\mathbb{R}^3), \qquad \boldsymbol{w}_{\delta_j} \to \boldsymbol{w} \text{ a.e.} \quad \text{and} \quad \liminf_{j\to\infty} E(\boldsymbol{w}_{\delta_j}) \ge F(\boldsymbol{w}). \tag{3.3}$$

By [9, Proposition 3.1], the inverse map $\boldsymbol{w}^{-1}$ belongs to BV. Let us see that it fails to be in a Sobolev space by estimating $\|D^s \boldsymbol{w}^{-1}\|$ from below. Indeed, by (3.3) and the boundary condition $\boldsymbol{w}_{\delta_j} = \boldsymbol{v}$ in $\Omega \setminus U_{\delta_j}$, we have that $\boldsymbol{w}$ coincides with $\boldsymbol{v}$ a.e. outside U, and, hence, outside the

half-ball a. Therefore, $\boldsymbol{w}^{-1}$ coincides with $\boldsymbol{v}^{-1}$ a.e. outside the ball $B((0,0,1/2),1/2)=\boldsymbol{v}(a)$. In particular, $\boldsymbol{w}^{-1}$ sends $\boldsymbol{v}(e)$ to e, so $\boldsymbol{w}^{-1}$ has also a discontinuity on Γ and the amplitude of the jump is at least 1 (the distance of the two half-balls a and e in the reference configuration). Then $\|D^s\boldsymbol{w}^{-1}\|\geq\pi$ and by (3.3)

$$\liminf_{j\to\infty} E(\boldsymbol{w}_{\delta_j})\geq E(\boldsymbol{w})+2\pi. \tag{3.4}$$

Using (3.1), we have that $\boldsymbol{w}\in\overline{\mathcal{A}^r_\delta}$ for all $\delta\in(0,1]$, so

$$\inf\{E(\boldsymbol{u})\colon \boldsymbol{u}\in\overline{\mathcal{A}^r_\delta}\}\leq E(\boldsymbol{w})$$

and, in particular,

$$\liminf_{j\to\infty}\inf\{E(\boldsymbol{u})\colon \boldsymbol{u}\in\overline{\mathcal{A}^r_{\delta_j}}\}\leq E(\boldsymbol{w}). \tag{3.5}$$

From (3.2) we obtain

$$\liminf_{j\to\infty} E(\boldsymbol{w}_{\delta_j})\leq\liminf_{j\to\infty}\inf\{E(\boldsymbol{u})\colon \boldsymbol{u}\in\overline{\mathcal{A}^r_{\delta_j}}\}+\lambda. \tag{3.6}$$

Combining (3.4), (3.5) and (3.6) we get a contradiction. □

4. Variants of Theorem 1.1

In this section we give two variants of our main Theorem 1.1, and of its version in Theorem 3.2, in which the infimum in the larger space is attained.

4.1. **The axisymmetric setting.** We first give a variant of Theorem 1.1 in the axisymmetric setting. For Ω and $\widetilde{\Omega}$ two smooth axisymmetric bounded open subsets of $\mathbb{R}^3$ such that $\widetilde{\Omega}\subset\subset\Omega$ and for $\boldsymbol{b}:\widetilde{\Omega}\to\mathbb{R}^3$ a bi-Lipschitz axisymmetric homeomorphism, we define

$$\mathcal{A}_s=\mathcal{A}_s(\Omega,\widetilde{\Omega},\boldsymbol{b}):=\{\boldsymbol{u}\in\mathcal{A}\colon \boldsymbol{u}\text{ is axisymmetric}\}\quad\text{ and }\quad\mathcal{A}^r_s:=\mathcal{A}_s\cap\mathcal{A}^r. \tag{4.1}$$

We denote by $\overline{\mathcal{A}}^r_s$ the weak sequential closure in H^1 of maps in $\mathcal{A}^r_s$. For the precise definition of axisymmetric maps we refer to [7, Section 2.3]. The variant of Theorems 1.1 and 3.2 in this context is as follows.

Theorem 4.1. *We assume that H is a convex function that satisfies conditions* (1.2) *and* (1.4). *Set $\Omega=B(\mathbf{0},4)$. Then for all $\lambda\in(0,2\pi)$ there exist an axisymmetric domain $\widetilde{\Omega}\subset\subset\Omega$ and a bi-Lipschitz axisymmetric homeomorphism $\boldsymbol{b}:\Omega\to\mathbb{R}^3$ such that*

$$\inf\{E(\boldsymbol{u}):\boldsymbol{u}\in\mathcal{A}^r_s\}\geq\min\{E(\boldsymbol{u}):\boldsymbol{u}\in\overline{\mathcal{A}}^r_s\}+\lambda \tag{4.2}$$

$$\geq\min\{E(\boldsymbol{u}):\boldsymbol{u}\in\mathcal{A}_s\}+\lambda. \tag{4.3}$$

Proof. The proof is exactly the same as the one of Theorem 3.2, with the same choices of $\widetilde{\Omega}=U_\delta$ and $\boldsymbol{b}=\boldsymbol{b}_\delta$. The key point is that the Conti–De Lellis map is axisymmetric and so is its patch obtained in Theorem 3.1. □

We note that the minima on the right-hand side of (4.2) and (4.3) are attained thanks to [7, Proposition 6.6 and Theorem 3.2].

4.2. **Working with the weak closure of Sobolev homeomorphisms.** In another direction, in a general non-axisymmetric setting, instead of working with $\mathcal{A}^r$ and its weak closure we can work with the class of Sobolev homeomorphisms and its weak closure. For Ω and $\widetilde{\Omega}$ two smooth bounded open subsets of $\mathbb{R}^3$ such that $\widetilde{\Omega}\subset\subset\Omega$ and for $\boldsymbol{b}:\widetilde{\Omega}\to\mathbb{R}^3$ a bi-Lipschitz homeomorphism we define

$$\mathcal{H}=\mathcal{H}(\Omega,\widetilde{\Omega},\boldsymbol{b}):=\{\boldsymbol{u}:\Omega\to\boldsymbol{b}(\Omega)\text{ homeomorphism satisfying Lusin's condition (N)},$$
$$\boldsymbol{u}=\boldsymbol{b}\text{ on }\Omega\setminus\widetilde{\Omega}\text{ and }E(\boldsymbol{u})\leq E(\boldsymbol{b})\}.$$

Recall that a map $\boldsymbol{u}:\Omega\to\mathbb{R}^3$ satisfies Lusin's condition (N) if $|\boldsymbol{u}(A)|=0$ for any $A\subset\mathbb{R}^3$ such that $|A|=0$. We denote by $\overline{\mathcal{H}}$ the weak closure in H^1 of maps in $\mathcal{H}(\Omega,\widetilde{\Omega},\boldsymbol{b})$. The variant of Theorems 1.1 and 3.2 in this context is as follows.

Theorem 4.2. *We assume that H is a convex function that satisfies conditions* (1.2) *and* (1.4). *Let $\Omega=B(\mathbf{0},4)$. Then for all $\lambda\in(0,2\pi)$ there exist a smooth open set $\widetilde{\Omega}\subset\subset\Omega$ and a bi-Lipschitz homeomorphism $\boldsymbol{b}:\Omega\setminus\widetilde{\Omega}\to\mathbb{R}^3$ such that*

$$\inf\{E(\boldsymbol{u}):\boldsymbol{u}\in\mathcal{H}\}\geq\min\{E(\boldsymbol{u}):\boldsymbol{u}\in\overline{\mathcal{H}}\}+\lambda. \tag{4.4}$$

Proof. The proof is again the same as in Theorem 3.2. The key points are that homeomorphisms satisfying Lusin's condition (N) in turn satisfy the divergence identities (see [27, Theorem 5.4]) and, hence, $\mathcal{H}\subset\mathcal{A}^r$, and that the patch of the Conti–De Lellis map $\boldsymbol{u}_\delta$ obtained in Theorem 3.1 is a bi-Lipschitz homeomorphism (and hence satisfies Lusin's condition). The minimum in the right-hand side of (4.4) is attained due to [28, Theorem 4.3]). □

Appendix A. The dipole map

The definition of the limiting map in the Conti–De Lellis example is constructed by partitioning the ball $B(\mathbf{0},3)$ into several distinct subregions. By axisymmetry, it suffices to describe $\boldsymbol{v}$ in the right half-plane. We describe $\boldsymbol{v}$ by using spherical coordinates $(v_\rho,v_\theta=\theta,v_\varphi)$ in the image. Note that, when $\theta=0$, the vector $\boldsymbol{e}_r$ equals $\boldsymbol{e}_1$; as a consequence, (v_ρ,v_φ) are the polar coordinates of the map $\boldsymbol{v}$ restricted to the plane generated by $(\boldsymbol{e}_1,\boldsymbol{e}_3)$.

Region $a:=\{\rho\sin\varphi\boldsymbol{e}_r(\theta)+\rho\cos\varphi\boldsymbol{e}_3:\ 0\leq\rho\leq1,\frac{\pi}{2}\leq\varphi\leq\pi\}$. In this region we set

$$\boldsymbol{v}\big(\rho\sin\varphi\boldsymbol{e}_r(\theta)+\rho\cos\varphi\boldsymbol{e}_3\big)=v_\rho\sin v_\varphi\,\boldsymbol{e}_r(\theta)+v_\rho\cos v_\varphi\,\boldsymbol{e}_3,$$
$$v_\rho(\rho,\varphi)=(1-\rho)\cos v_\varphi,\qquad v_\varphi(\rho,\varphi)=\pi-\varphi.$$

Region $b:=\{\rho\sin\varphi\boldsymbol{e}_r(\theta)+\rho\cos\varphi\boldsymbol{e}_3:1<\rho\leq3,\frac{\pi}{2}\leq\varphi\leq\pi\}$. Here we define $\boldsymbol{v}$ by

$$\boldsymbol{v}\big(\rho\sin\varphi\,\boldsymbol{e}_r(\theta)+\rho\cos\varphi\,\boldsymbol{e}_3\big)=v_\rho\sin v_\varphi\,\boldsymbol{e}_r(\theta)+v_\rho\cos v_\varphi\,\boldsymbol{e}_3,$$
$$v_\rho(\rho,\varphi)=\rho-1,\qquad v_\varphi(\rho,\varphi)=\frac{\varphi+\pi}{2}.$$

Region $e:=\{\rho\sin\varphi\boldsymbol{e}_r(\theta)+(1+\rho\cos\varphi)\boldsymbol{e}_3:0\leq\rho\leq1,0\leq\varphi\leq\frac{\pi}{2}\}$. Here we set

$$\boldsymbol{v}\big(\boldsymbol{e}_3+\rho\sin\varphi\boldsymbol{e}_r(\theta)+\rho\cos\varphi\boldsymbol{e}_3\big):=v_\rho\sin\varphi\,\boldsymbol{e}_r(\theta)+v_\rho\cos\varphi\,\boldsymbol{e}_3,$$
$$v_\rho(\rho,\varphi):=(1+\rho)\cos\varphi,\quad v_\varphi=\varphi.$$

Region $f:=\{\boldsymbol{e}_3+\rho\sin\varphi\boldsymbol{e}_r(\theta)+\rho\cos\varphi\boldsymbol{e}_3:\rho\geq1,0\leq\varphi\leq\frac{\pi}{2}\}\cap B(\mathbf{0},3)$. In the original construction provided by [13], the only requirements are that:

- The 2D representative of

  $$\boldsymbol{v}\big(\boldsymbol{e}_3+\rho\sin\varphi\boldsymbol{e}_r(\theta)+\rho\cos\varphi\boldsymbol{e}_3\big)=v_\rho\sin v_\varphi\boldsymbol{e}_r(\theta)+v_\rho\cos v_\varphi\boldsymbol{e}_3,\quad\rho\geq1,\ \varphi\in[0,\frac{\pi}{2}],$$

  sends the 2D region

  $$\{(\rho\sin\varphi,1+\rho\cos\varphi):\rho\geq1,0\leq\varphi\leq\frac{\pi}{2}\}\cap B\big((0,0),3\big)$$

  in a bi-Lipschitz manner onto its image, which is contained in

  $$\{(v_\rho\sin v_\varphi,v_\rho\cos v_\varphi):v_\rho\geq2\cos v_\varphi,\ 0\leq v_\varphi\leq\frac{\pi}{2}\}.$$

- The map $\boldsymbol{v}$ matches the definition of region e at the interface:

  $$v_\rho(1,\varphi):=2\cos\varphi,\qquad v_\varphi(1,\varphi):=\varphi.$$

  In particular, $v_\rho(1,\frac{\pi}{2})=0$.

- The map $\boldsymbol{v}$ sends the half-line $\{(\rho, \frac{\pi}{2}) : \rho \geq 1\}$ to the ray $\{\varphi = \frac{\pi}{2}\}$:

$$v_\varphi(\rho, \frac{\pi}{2}) = \frac{\pi}{2}, \qquad \rho \geq 1.$$

Here, we simply use

$$v_\rho(\rho, \varphi) = 2\cos\varphi + (\rho - 1), \qquad v_\varphi(\rho, \varphi) = \varphi. \tag{A.1}$$

Region $d := \{0 \leq x_3 \leq 1\} \cap B(\mathbf{0}, 3)$. In [13] the limit map $\boldsymbol{v}$ is defined as the composition of two maps. The first one is an auxiliary generic axisymmetric

$$\boldsymbol{g}\big(\boldsymbol{x}\big) = s(r, x_3)\, \boldsymbol{e}_r(\theta) + z(r, x_3)\, \boldsymbol{e}_3, \qquad \boldsymbol{x} = r\boldsymbol{e}_r + x_3\boldsymbol{e}_3, \tag{A.2}$$

whose planar representative is a bi-Lipschitz transformation from the 2D region

$$\{(r, x_3) :\ r \geq 0,\ 0 \leq x_3 \leq 1,\ r^2 + x_3^2 < 3^2\}$$

onto its image, which is contained in

$$\{(s, z) :\ s \geq 0,\ 0 \leq z \leq 3\}.$$

This transformation $\boldsymbol{g}$ is then composed with the transformation from the cylindrical coordinates (s, z) to the spherical coordinates $(s, \varphi(z))$:

$$\boldsymbol{v}\big(r\boldsymbol{e}_r(\theta) + x_3\, \boldsymbol{e}_3\big) = s\, \sin\big(\varphi(z)\big)\, \boldsymbol{e}_r(\theta) - s\, \cos\big(\varphi(z)\big)\, \boldsymbol{e}_3, \tag{A.3}$$

with

$$\varphi(z) := \frac{\pi}{4}\bigg(1 + \frac{z}{3}\bigg).$$

As a result, the region d is mapped to the sector $\frac{\pi}{4} \leq \varphi \leq \frac{\pi}{2}$ in spherical coordinates (see Figure 1).

The transformation $\boldsymbol{g}$ must fulfill the following requirements:

- The points

$$A(r = 1, x_3 = 0), \quad B(r = 0, x_3 = 0), \quad C(r = 0, x_3 = 1), \quad D(r = 1, x_3 = 1),$$

respectively, are mapped to

$$(s = 0, z = 0), \quad (s = 0, z = 1), \quad (s = 0, z = 2), \quad (s = 0, z = 3).$$

In the segments joining those points, $\boldsymbol{g}$ is affine. (After composing with the polar transformation $s\sin\varphi\, \boldsymbol{e}_r - s\cos\varphi\, \boldsymbol{e}_3$, the polygonal curve $ABCD$ is contracted to a point.)

- At the interface $\{r \geq 1,\ x_3 = 1\}$,

$$s(r, 1) := v_\rho(r, \frac{\pi}{2}), \quad z(r, 1) \equiv 3, \tag{A.4}$$

where $v_\rho(r, \varphi)$ is the radial spherical coordinate of the image in region f. In this article we choose a particular definition of this function, namely, the one in (A.1). Hence, (A.4) becomes

$$s(r, 1) := r - 1, \quad z(r, 1) \equiv 3.$$

- At the interface $\{r \geq 1, x_3 = 0\}$

$$s(r, 0) := r - 1, \quad z(r, 0) \equiv 0.$$

This is consistent with the definition of the dipole in region b.

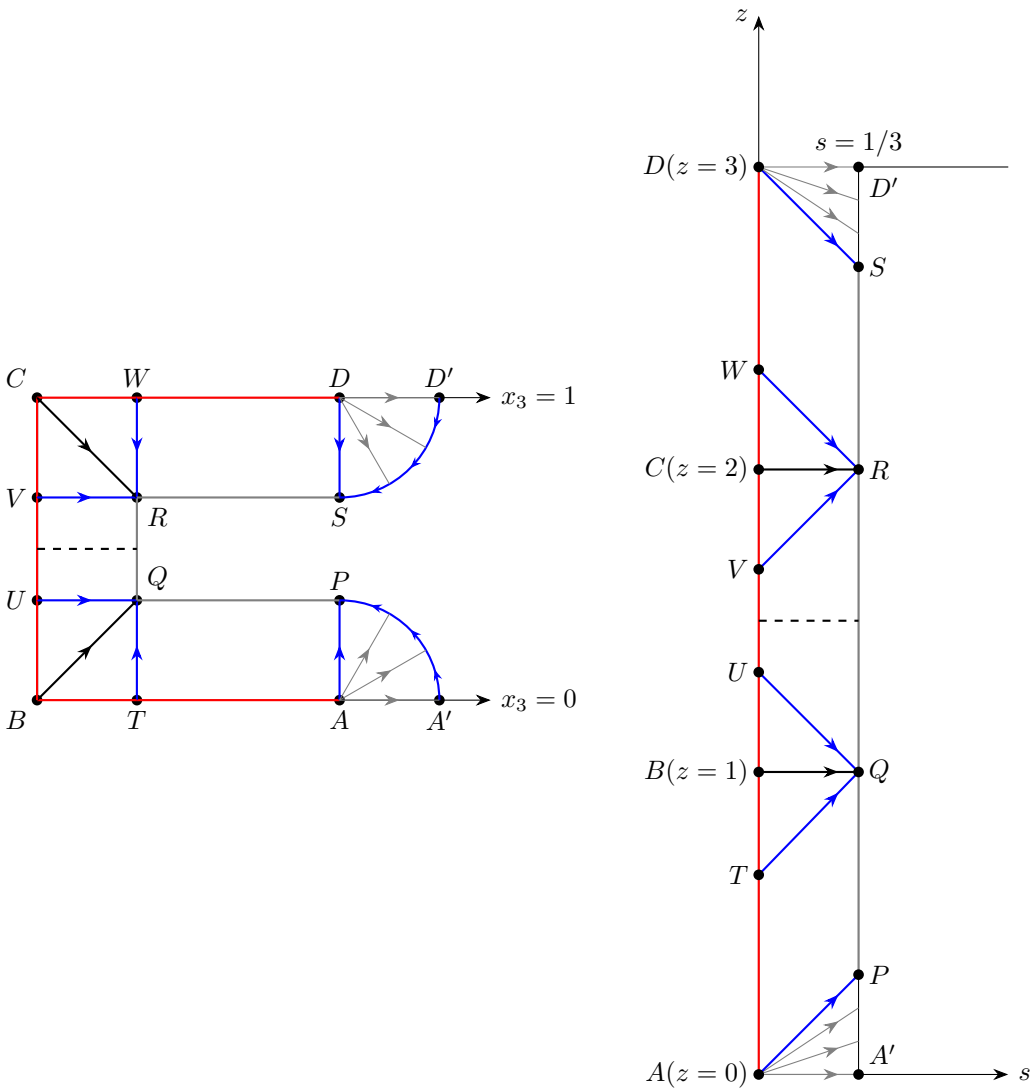


FIGURE 4. The transformation $\boldsymbol{g} = s(r, x_3)\boldsymbol{e}_r + z(r, x_3)\boldsymbol{e}_3$ from the (planar representative slice of) region d in the reference configuration (left) onto the intermediate (s, z) configuration (right).

In [13, 8] there is flexibility regarding the way to define $\boldsymbol{g}$ in the interior of the slab. Here we are going to use a specific function $\boldsymbol{g}$ (see Figure 4) whose radial coordinate $s(r, x_3)$ is given exactly by

$$s = \operatorname{dist}(\boldsymbol{x}, U), \quad \boldsymbol{x} = r\boldsymbol{e}_r + x_3\boldsymbol{e}_3 \tag{A.5}$$

in the subregion $\{\boldsymbol{x} : 0 \le \operatorname{dist}(\boldsymbol{x}, U) \le \frac{1}{3}\}$.

Bounds on the Jacobian. Throughout the rest of the paper, c will denote a universal positive constant whose precise value may change from line to line. We will also use the following elementary result.

Lemma A.1. *If $H : (0, \infty) \to \mathbb{R}$ is convex and $\lim_{s\to 0} H(s) = \infty$ then there exists $\delta > 0$ such that H is decreasing in $(0, \delta)$.*

Proof. As H is convex, its right derivative H'_+ exists everywhere on $(0,\infty)$ and is non-decreasing. Then the limit $\lim_{s\to 0} H'_+(s)$ exists, and must be $-\infty$ since $\lim_{s\to 0} H(s) = \infty$. Therefore, H'_+ is negative in $(0,\delta)$ for some $\delta > 0$. □

In region d we have[1]

$$\det D\boldsymbol{v}(\boldsymbol{x}) = \frac{s^2(r,x_3)\sin\varphi(z(r,x_3))}{r} \geq \frac{\sqrt{2}}{2}\frac{s^2}{r}$$

since $\frac{\pi}{4} \leq \varphi \leq \frac{\pi}{2}$. This determinant goes to zero as $\boldsymbol{x}$ approaches the polygonal line $ABCD$ on ∂U. Focusing on the region where $s \leq \frac{1}{3}$ (see Figure 4), we have that $r \leq \frac{4}{3}$ and, hence, $\det D\boldsymbol{v} \geq c\, s^2$. By symmetry with respect to the plane $\{x_3 = \frac{1}{2}\}$, it is enough to consider $\boldsymbol{x} = r\boldsymbol{e}_r + x_3\boldsymbol{e}_3$ with $x_3 \in [\frac{1}{2}, 1]$. Here one has

$$\operatorname{dist}(\boldsymbol{x}, U) \geq \min\{r,\, 1 - x_3\},$$

since the distance from $\boldsymbol{x}$ to the axis is r, while the distance from $\boldsymbol{x}$ to the top disk $\{x_3 = 1,\ 0 \leq r \leq 1\}$ is at least $1 - x_3$. Hence, by (A.5), we have

$$\det D\boldsymbol{v}(\boldsymbol{x}) \geq c\, s^2(r,x_3) \geq c\, \min\{r^2,\, (1-x_3)^2\}.$$

Using that H is decreasing near 0, and using (1.4), we obtain

$$H(\det D\boldsymbol{v}(\boldsymbol{x})) \leq c\, \min\{r^2,\, (1-x_3)^2\}^{-\alpha} \leq c\Big(r^{-2\alpha} + (1-x_3)^{-2\alpha}\Big).$$

Therefore,

$$\int_{\{s\leq\frac{1}{3}\}} H(\det D\boldsymbol{v})\,\mathrm{d}\boldsymbol{x} \leq c\int_0^{4/3}\int_{1/2}^1 \Big(r^{-2\alpha} + (1-x_3)^{-2\alpha}\Big)\, 2\pi r\,\mathrm{d}x_3\mathrm{d}r, \tag{A.6}$$

i.e., in this region $H(\det D\boldsymbol{v})$ is integrable if $\alpha < \frac{1}{2}$.

In region e we have $v_\varphi = \varphi$ and $v_\rho(\rho,\varphi) = (1+\rho)\cos\varphi$, so that $\partial_\rho v_\rho = \cos\varphi$ and[2]

$$\det D\boldsymbol{v} = \frac{v_\rho^2}{\rho^2}\,\partial_\rho v_\rho = \frac{(1+\rho)^2\cos^3\varphi}{\rho^2}\,.$$

This determinant is close to zero near the interface with region d (particularly at the triple junction, where $\rho \approx 1$ and $\cos\varphi \approx 0$) and unbounded near the cavitation point $\mathbf{0}' = (0,0,1)$, where $\rho \to 0^+$. To estimate the integral of $H(\det D\boldsymbol{v})$ we split region e into $\{\det D\boldsymbol{v} \leq 1\}$ and $\{\det D\boldsymbol{v} > 1\}$. On the first set the growth condition (1.4) gives $H(t) \leq c\, t^{-\alpha}$ for all $t \in (0,1]$ (after adjusting the constant c, since H is continuous on $(0,\infty)$), while on the second set $H(t) \leq c\, t^\beta$ for all $t \geq 1$. Writing the volume element in spherical coordinates as $\mathrm{d}\boldsymbol{x} = 2\pi\,\rho^2\sin\varphi\,\mathrm{d}\rho\,\mathrm{d}\varphi$ and enlarging each integral to the full region e, we obtain

$$\begin{aligned}\int_{\{\det D\boldsymbol{v}\leq 1\}\cap e} H(\det D\boldsymbol{v})\,\mathrm{d}\boldsymbol{x} &\leq c\int_0^{\pi/2}\int_0^1 \Big(\frac{(1+\rho)^2\cos^3\varphi}{\rho^2}\Big)^{-\alpha}\rho^2\sin\varphi\,\mathrm{d}\rho\,\mathrm{d}\varphi \\ &= c\int_0^{\pi/2}\cos^{-3\alpha}\varphi\,\sin\varphi\,\mathrm{d}\varphi\;\cdot\;\int_0^1 (1+\rho)^{-2\alpha}\rho^{2+2\alpha}\mathrm{d}\rho\,,\end{aligned}$$

[1] See, e.g., [8, Appendix B.4] for the computation of the determinant of a map expressed in cylindrical-spherical coordinates.

[2] See, e.g., [8, Appendix B.3] for the computation of the determinant of a map expressed in spherical-spherical coordinates.

and

$$\int_{\{\det D\boldsymbol{v}>1\}\cap e} H(\det D\boldsymbol{v})\,\mathrm{d}\boldsymbol{x} \le c\int_0^{\pi/2}\!\!\int_0^1 \Big(\frac{(1+\rho)^2\cos^3\varphi}{\rho^2}\Big)^{\beta}\rho^2\sin\varphi\,\mathrm{d}\rho\,\mathrm{d}\varphi$$
$$= c\int_0^{\pi/2}\cos^{3\beta}\varphi\ \sin\varphi\,\mathrm{d}\varphi\ \cdot\ \int_0^1 (1+\rho)^{2\beta}\rho^{2-2\beta}\mathrm{d}\rho\,.$$

Both right-hand sides are finite under condition (1.4) with $\alpha < 1/3$ and $\beta < 3/2$, so $H(\det D\boldsymbol{v})$ is integrable in region e.

One can check that in the remaining regions the integrability of the Jacobian is not worse (for more details, see [8, Section 3]).

Appendix B. The approximating sequence

We recall from [8, Theorem 1.2] that for every sufficiently small $\varepsilon > 0$ there exists an axisymmetric map $\boldsymbol{u}_\varepsilon \in \mathcal{A}^r$ with the following properties:

(i) $\boldsymbol{u}_\varepsilon$ is a bi-Lipschitz homeomorphism of $B(\mathbf{0},4)$, orientation preserving, and coincides with the identity on $\partial B(\mathbf{0},4)$;
(ii) $\boldsymbol{u}_\varepsilon \rightharpoonup \boldsymbol{v}$ in $H^1(B(\mathbf{0},4),\mathbb{R}^3)$ and a.e. in $B(\mathbf{0},4)$;
(iii) the energies are uniformly bounded, i.e.,

$$\sup_{\varepsilon>0} E(\boldsymbol{u}_\varepsilon) < \infty.$$

The approximation $\boldsymbol{u}_\varepsilon$ is defined (in the regions of our interest) as follows. We refer to [8] for the full construction. From now on, a choice is made of

$$0 < \gamma \le \frac{1}{3}, \quad \text{a fixed positive exponent.}$$

This range for γ played an important role in [8] in order to show that $\boldsymbol{u}_\varepsilon$ is an approximating sequence for the dipole $\boldsymbol{v}$ with optimal energy (compare with (B.9)). The fixed region labels refer to the reference configuration in Figure 1; the ε-dependent regions of the approximating maps are shown in Figure 2.

Region b. We work with spherical coordinates (ρ,θ,φ), $1<\rho<3,\ 0\le\theta<2\pi,\ \pi/2\le\varphi\le\pi$ in the reference configuration and cylindrical coordinates in the deformed configuration. We first define the auxiliary functions

$$\boldsymbol{d}(\varphi,\theta) := \sin\left(\frac{\varphi+\pi}{2}\right)\boldsymbol{e}_r(\theta) + \cos\left(\frac{\varphi+\pi}{2}\right)\boldsymbol{e}_3,$$

$$\boldsymbol{\phi}_\varepsilon(\boldsymbol{x}) := (\rho - 1 + \sqrt{2}\,\varepsilon^\gamma)\,\boldsymbol{d}(\varphi,\theta) + \varepsilon^\gamma\,\boldsymbol{e}_3.$$

With this notation, we have $\boldsymbol{v}(\boldsymbol{x}) = (\rho-1)\,\boldsymbol{d}(\varphi,\theta)$. The factor $\sqrt{2}$ appears because, according to the definition of $\boldsymbol{u}_\varepsilon$ in region a_ε, the image of A is $(\varepsilon^\gamma,0)$, whose distance to $(0,\varepsilon^\gamma)$ is $\sqrt{2}\varepsilon^\gamma$. In region b we define $\boldsymbol{u}_\varepsilon$ to be

$$\boldsymbol{u}_\varepsilon(\boldsymbol{x}) = \varepsilon^\gamma\boldsymbol{\psi}\Big(\varepsilon^{-\gamma}\boldsymbol{\phi}_\varepsilon(\boldsymbol{x})\Big), \tag{B.1}$$

where $\boldsymbol{\psi}$ is any axisymmetric bi-Lipschitz bijection from

$$\Big\{(x_1,x_2,x_3):\ r^2+(x_3-1)^2\ge 2,\ x_3\le 0,\ r\le 1+|x_3|\Big\}$$

onto

$$\Big\{(x_1,x_2,x_3):\ x_3\le 0,\ r\le 1+|x_3|\Big\}\cup B\big((0,0,0),\,1\big)$$

such that

i) $\boldsymbol{\psi}(r,x_3)=(r,x_3)$ on the half-line $r=1+|x_3|$, $x_3\le 0$,
ii) $\boldsymbol{\psi}\big(\sqrt{2}\sin(\bar\varphi),1+\sqrt{2}\cos(\bar\varphi)\big)=\Big(\sin\big(2(\pi-\bar\varphi)\big),\cos\big(2(\pi-\bar\varphi)\big)\Big)$, $\frac{3\pi}{4}\le\bar\varphi\le\pi$,
iii) $\boldsymbol{\psi}\equiv\mathbf{id}$ in $\{\boldsymbol{x}:\ r^2+(x_3-1)^2\ge 8,\ x_3\le 0,\ r\le 1+|x_3|\}$.

Region $e_\varepsilon:=\{\boldsymbol{e}_3+\rho\sin\varphi\boldsymbol{e}_r(\theta)+\rho\cos\varphi\boldsymbol{e}_3:\ \varepsilon<\rho<1,\ 0\le\varphi\le\frac{\pi}{2}\}$. Here we define $\boldsymbol{u}_\varepsilon$ in region e_ε through its spherical coordinates

$$u^\varepsilon_\varphi(\rho,\varphi):=\varphi,\qquad u^\varepsilon_\rho(\rho,\varphi):=\frac{1-\rho}{1-\varepsilon}u^\varepsilon_\rho(\varepsilon,\varphi)+\frac{\rho-\varepsilon}{1-\varepsilon}(2\cos\varphi+6\varepsilon^\gamma),$$

$$u^\varepsilon_\rho(\varepsilon,\varphi)=\left((\cos\varphi+2\varepsilon^\gamma)^3+\left[\frac{3r}{\partial_r\big(-\cos f(r)\big)}\right]_{r=g_\varepsilon(\varphi)}+3\int_{s=0}^{1}h_\varepsilon(s,\varphi)\mathrm{d}s\right)^{\frac{1}{3}},$$

the function $h_\varepsilon(s,\varphi)$ being defined by

$$h_\varepsilon(s,\varphi):=\varepsilon\Big((1-s)\frac{g_\varepsilon(\varphi)}{\sin\varphi}+s\varepsilon\Big)\Big((1-s)g_\varepsilon'(\varphi)\cos\varphi+s(\varepsilon-g_\varepsilon(\varphi)\sin\varphi)\Big),\tag{B.2}$$

with $g_\varepsilon:[0,\frac{\pi}{2}]\to[0,\varepsilon]$ the inverse of the function f_ε defined by

$$f_\varepsilon(r):=\arctan\left(\frac{r}{\varepsilon^2}\right)+\alpha_\varepsilon\frac{r}{\varepsilon},\quad 0\le r\le\varepsilon,\qquad \alpha_\varepsilon:=\arctan(\varepsilon).\tag{B.3}$$

Region f. We define $\boldsymbol{u}_\varepsilon$ through its spherical coordinates

$$u^\varepsilon_\rho(\rho,\varphi):=2\cos\varphi+\rho-1+6\varepsilon^\gamma,\qquad u^\varepsilon_\varphi(\rho,\varphi):=\varphi.$$

Note that when $\rho=1$ the radial coordinate

$$u^\varepsilon_\rho(1,\varphi)=2\cos\varphi+6\varepsilon^\gamma$$

coincides with the definition given in region e_ε.

Region $d_\varepsilon:=\{x_1^2+x_2^2>\varepsilon^2,\ 0<x_3<1\}$. We use cylindrical coordinates in the domain. The approximating map

$$\boldsymbol{u}_\varepsilon\big(r\boldsymbol{e}_r(\theta)+x_3\boldsymbol{e}_3\big)=\boldsymbol{w}_\varepsilon\Big(\boldsymbol{g}\big(\hat r\boldsymbol{e}_r(\theta)+x_3\,\boldsymbol{e}_3\big)\Big)=w^\varepsilon_r(s,z)\boldsymbol{e}_r(\theta)+w^\varepsilon_3(s,z)\,\boldsymbol{e}_3,\tag{B.4}$$

is defined by composing three different auxiliary transformations. The first one is given by

$$\hat r=\begin{cases}\dfrac{(r-\varepsilon)r}{\varepsilon^{2\gamma}-\varepsilon}, & \varepsilon<r\le\varepsilon^{2\gamma},\\ r, & r\ge\varepsilon^{2\gamma}.\end{cases}\tag{B.5}$$

After this transformation the radial distance lies in the same interval $(0,\infty)$ for all ε. The second transformation is the fixed axisymmetric map

$$\boldsymbol{g}(\hat r\boldsymbol{e}_r(\theta)+x_3\boldsymbol{e}_3)=s(\hat r,x_3)\boldsymbol{e}_r+z(\hat r,x_3)\boldsymbol{e}_3$$

used before in region d. The third transformation is

$$\begin{aligned}&\boldsymbol{w}_\varepsilon\big(s\,\boldsymbol{e}_r(\theta)+z\,\boldsymbol{e}_3\big)=w^\varepsilon_r(s,z)\,\boldsymbol{e}_r(\theta)+w^\varepsilon_3(s,z)\,\boldsymbol{e}_3\\ &w^\varepsilon_r(s,z)=\omega_\varepsilon(z)+s\,\sin\big(\varphi(z)\big),\\ &w^\varepsilon_3(s,z)=-s\,\cos\big(\varphi(z)\big),\end{aligned}\qquad\text{with}\quad\varphi(z):=\tfrac{\pi}{4}\left(1+\tfrac{z}{3}\right).\tag{B.6}$$

The function $\omega_\varepsilon:[0,3]\to\mathbb{R}$ in (B.6) is defined as

$$\omega_\varepsilon(z)=\begin{cases}z(2\varepsilon^\gamma)+(1-z)\varepsilon^\gamma, & 0\le z\le 1,\\ \left((2\varepsilon^\gamma)^3+(z-1)\cdot\dfrac{3\varepsilon}{f_\varepsilon'(\varepsilon)}\right)^{1/3}, & 1\le z\le 2,\\ (3-z)\eta_\varepsilon+(z-2)(6\varepsilon^\gamma), & 2\le z\le 3,\end{cases}$$

with f_ε defined in (B.3). Notice that it is piecewise C^1 and

$$\omega_\varepsilon(0) = \varepsilon^\gamma, \quad \omega_\varepsilon(1) = 2\varepsilon^\gamma, \quad \omega_\varepsilon(2) = \eta_\varepsilon = 2\varepsilon^\gamma + o(\varepsilon^\gamma), \quad \omega_\varepsilon(3) = 6\varepsilon^\gamma.$$

Also, $\omega_\varepsilon(z)$ is increasing and, because of that,

$$\varepsilon^\gamma \le \omega_\varepsilon(z) \le 6\varepsilon^\gamma \quad \text{for all } z \in [0,3]. \tag{B.7}$$

In addition, as mentioned in [8, Section 3.3.8], using that $\gamma \le \frac{1}{3}$ it can be checked that

$$|\omega_\varepsilon'(z)| \le c\,\varepsilon^\gamma \qquad \text{for all } z \in [0,3]. \tag{B.8}$$

The definition of $\boldsymbol{u}_\varepsilon$ matches the one already provided in regions a_ε, b, c_ε, e_ε, and f. In particular,

- On the interface between d_ε and b, the deformation $\boldsymbol{u}_\varepsilon$ is:

$$r \ge 1 \quad \Rightarrow \quad \boldsymbol{u}_\varepsilon\big(r\,\boldsymbol{e}_r(\theta)\big) = \varepsilon^\gamma \boldsymbol{e}_r(\theta) + (r-1)\frac{\boldsymbol{e}_r(\theta) - \boldsymbol{e}_3}{\sqrt{2}}.$$

- On the interface between e_ε and d_ε, the deformation is:

$$\varepsilon \le r \le 1 \;\Rightarrow\; \boldsymbol{u}_\varepsilon\big(\boldsymbol{e}_3 + r\,\boldsymbol{e}_r(\theta)\big) = \left(\frac{1-r}{1-\varepsilon}\eta_\varepsilon + \frac{r-\varepsilon}{1-\varepsilon}6\varepsilon^\gamma\right)\boldsymbol{e}_r(\theta),$$

  with

$$\begin{aligned}\eta_\varepsilon :=& u_\rho^\varepsilon(\varepsilon, \frac{\pi}{2}) = \left((2\varepsilon^\gamma)^3 + \frac{3r}{\sin f_\varepsilon(r) f_\varepsilon'(r)}\bigg|_{r=\varepsilon}\right)^{\frac{1}{3}} = \left((2\varepsilon^\gamma)^3 + \frac{3\varepsilon}{f_\varepsilon'(\varepsilon)}\right)^{\frac{1}{3}} \\ =& 2\varepsilon^\gamma + o(\varepsilon^\gamma).\end{aligned} \tag{B.9}$$

  This relevant quantity η_ε is of order ε^γ (this is why we chose $\gamma \le 1/3$).
- On the interface with f, the deformation is prescribed to be

$$r \ge 1 \quad \Rightarrow \quad \boldsymbol{u}_\varepsilon\big(\boldsymbol{e}_3 + r\,\boldsymbol{e}_r(\theta)\big) = \big(r - 1 + 6\varepsilon^\gamma\big)\,\boldsymbol{e}_r(\theta).$$

Energy bounds. In [8, Section 3.3.3] it is shown that in those parts of the domain where $\det D\boldsymbol{v}$ is close to zero, a lower bound of the form

$$\det D\boldsymbol{u}_\varepsilon(\boldsymbol{x}) \ge c \det D\boldsymbol{v}(\boldsymbol{x})$$

holds. Because of that, the energy of $\boldsymbol{u}_\varepsilon$ is controlled.

Remark B.1 (The scale ε^γ). In the construction we fixed an exponent $0 < \gamma \le \frac{1}{3}$ and we repaired the singular behavior of $\boldsymbol{v}$ by *opening* the collapsed set (the axis/neck) at a small geometric scale of order ε^γ.

More precisely, the maps $\boldsymbol{u}_\varepsilon$ coincide with $\boldsymbol{v}$ away from the singular set, but differ from $\boldsymbol{v}$ by shifts/extrusions whose amplitude is $\sim \varepsilon^\gamma$:

- in region b, the auxiliary map $\boldsymbol{\phi}_\varepsilon$ differs from $\boldsymbol{v}$ by the translations $\sqrt{2}\,\varepsilon^\gamma$ along the direction $\boldsymbol{d}(\varphi,\theta)$ and ε^γ in the $\boldsymbol{e}_3$–direction (see (B.1));
- in the neck d_ε, the "horizontal extrusion" function satisfies $\varepsilon^\gamma \le \omega_\varepsilon(z) \le 6\varepsilon^\gamma$ for all $z \in [0,3]$ (see (B.7)), so that the radius of the opened tube is comparable to ε^γ;
- the matching radius at the interface between e_ε and d_ε is $\eta_\varepsilon = 2\varepsilon^\gamma + o(\varepsilon^\gamma)$ (see (B.9)), which is the reason for the restriction $\gamma \le \frac{1}{3}$ in [8].

Appendix C. Patch of the dipole

We provide here the detailed construction of the maps $\boldsymbol{b}_\delta$ provided in Theorem 3.1 and the estimate of their energy.

Proof of Theorem 3.1. Given the complexity of the proof, we first outline our overall strategy.

(i) **Starting point:** The Conti–De Lellis dipole $\boldsymbol{v}$ is a singular map that fails to be one-to-one only on the boundary of the "bad" set U. Outside any neighborhood U_δ of U, the map $\boldsymbol{v}$ is a bi-Lipschitz homeomorphism onto its image. By the construction in [8] recalled in the Appendix B, there exist regular approximations $\boldsymbol{u}_\varepsilon \in \mathcal{A}^r$ with uniformly bounded energy, i.e., $\sup_{\varepsilon>0} E(\boldsymbol{u}_\varepsilon) < \infty$.

(ii) **Definition of $\boldsymbol{b}_\delta$:** For each $\delta \in (0,1]$, we choose $\varepsilon > 0$ sufficiently small so that $\delta \geq c_0 \varepsilon^\gamma$ for a constant c_0 large enough. The scale ε^γ is related to the energy concentration produced by $\boldsymbol{v}$; see Remark B.1. Then we define

$$\boldsymbol{b}_\delta(\boldsymbol{x}) := \begin{cases} \boldsymbol{u}_\varepsilon(\boldsymbol{x}) & \text{if } \operatorname{dist}(\boldsymbol{x}, U) \leq \delta/2, \\ \text{interpolation} & \text{if } \delta/2 \leq \operatorname{dist}(\boldsymbol{x}, U) \leq \delta, \\ \boldsymbol{v}(\boldsymbol{x}) & \text{if } \operatorname{dist}(\boldsymbol{x}, U) \geq \delta. \end{cases} \tag{C.1}$$

The key point is that the interpolation introduces gradient perturbations of order $\varepsilon^\gamma/\delta$, which remain controlled thanks to the scaling $\delta \geq c_0 \varepsilon^\gamma$.

The transition layer $T_\delta := U_\delta \setminus U_{\delta/2}$ is handled separately in each of the regions b, d, e, and f, using interpolations adapted to the local geometry and coordinate systems.

(iii) **Verification:** We show that $\boldsymbol{b}_\delta$ is continuous across all the interfaces, bi-Lipschitz and orientation-preserving (by checking $\det D\boldsymbol{b}_\delta > 0$ in each region), and has energy bounded independently of δ.

We now proceed with the detailed construction.

Fix $\delta \in (0,1]$ and let $U_\delta := \{\boldsymbol{x} \in B(\boldsymbol{0}, 4) \colon \operatorname{dist}(\boldsymbol{x}, U) < \delta\}$ as in the statement (see Figure 3). Let $0 < \gamma \leq 1/3$ be the exponent used in the definition of the approximating maps $\boldsymbol{u}_\varepsilon$ in the Appendix B.

Step 1: definition of $\boldsymbol{b}_\delta$.

In this step we define $\boldsymbol{b}_\delta$ in the transition layer

$$T_\delta := U_\delta \setminus U_{\delta/2} = \{\boldsymbol{x} \in B(\boldsymbol{0}, 4) \colon \delta/2 \leq \operatorname{dist}(\boldsymbol{x}, U) \leq \delta\}.$$

We choose $\varepsilon = \varepsilon(\delta) > 0$ so that

$$\delta \geq c_0 \, \varepsilon^\gamma \tag{C.2}$$

for a suitable constant c_0 that we tune along the construction. In the rest of the proof we abbreviate $\boldsymbol{u} := \boldsymbol{u}_\varepsilon$. Let $\chi_\delta : [0, \infty) \to [0, 1]$ be the scalar cut-off function defined by

$$\chi_\delta(t) := \begin{cases} 1, & 0 \leq t \leq \delta/2, \\ \dfrac{\delta - t}{\delta/2}, & \delta/2 \leq t \leq \delta, \\ 0, & t \geq \delta. \end{cases}$$

Notice the scale that governs the choice of $\varepsilon = \varepsilon(\delta)$ in the patching: in the transition layer T_δ the cut-off produces gradient terms of the form $(\boldsymbol{u}_\varepsilon - \boldsymbol{v}) \otimes \nabla \chi_\delta$. Since $|\nabla \chi_\delta| \sim \delta^{-1}$ and $|\boldsymbol{u}_\varepsilon - \boldsymbol{v}| \sim \varepsilon^\gamma$ on the relevant interfaces, the perturbation is of size $\varepsilon^\gamma/\delta$. The compatibility condition (C.2) is therefore the natural requirement ensuring that the interpolation does not create excessive strains and that the Jacobian remains positive throughout T_δ.

We define $\boldsymbol{b}_\delta$ separately in the four regions b, d, e, and f.

Transition layer in region b.

In spherical coordinates, region b is given by

$$\{\, \boldsymbol{x} = \rho \sin\varphi\, \boldsymbol{e}_r(\theta) + \rho\cos\varphi\, \boldsymbol{e}_3 :\ 1 < \rho \le 3,\ \tfrac{\pi}{2} \le \varphi \le \pi \,\},$$

and $\operatorname{dist}(\boldsymbol{x}, U) = \rho - 1$. Set $s := \rho - 1$ and recall from Appendix B the auxiliary maps used in the definition of $\boldsymbol{u}$ in region b:

$$\boldsymbol{d}(\varphi,\theta) = \sin\left(\frac{\varphi+\pi}{2}\right)\, \boldsymbol{e}_r(\theta) + \cos\left(\frac{\varphi+\pi}{2}\right)\, \boldsymbol{e}_3,$$

$$\boldsymbol{\phi}_\varepsilon(\boldsymbol{x}) = (s + \sqrt{2}\,\varepsilon^\gamma)\, \boldsymbol{d}(\varphi,\theta) + \varepsilon^\gamma\, \boldsymbol{e}_3.$$

In this region $\boldsymbol{v}(\boldsymbol{x}) = s\, \boldsymbol{d}(\varphi,\theta)$. Moreover, $\boldsymbol{v}$ and $\boldsymbol{u} = \boldsymbol{u}_\varepsilon$ have angular component $\frac{\varphi+\pi}{2}$.

We define $\boldsymbol{b}_\delta$ on $b \cap T_\delta$ (i.e., for $\delta/2 \le s \le \delta$) by cutting off exactly the two ε^γ–shifts that distinguish $\boldsymbol{\phi}_\varepsilon$ from $\boldsymbol{v}$:

$$\boldsymbol{b}_\delta(\boldsymbol{x}) := s\, \boldsymbol{d}(\varphi,\theta) + \chi_\delta(s)\Big(\sqrt{2}\,\varepsilon^\gamma\, \boldsymbol{d}(\varphi,\theta) + \varepsilon^\gamma\, \boldsymbol{e}_3\Big) = \big(s + \chi_\delta(s)\sqrt{2}\,\varepsilon^\gamma\big)\boldsymbol{d}(\varphi,\theta) + \chi_\delta(s)\varepsilon^\gamma\, \boldsymbol{e}_3.$$

Then $\boldsymbol{b}_\delta = \boldsymbol{v}$ on $\{s = \delta\}$ (since $\chi_\delta(\delta) = 0$). Also, on $\{s = \delta/2\}$ we have $\chi_\delta(\delta/2) = 1$ and hence $\boldsymbol{b}_\delta = \boldsymbol{\phi}_\varepsilon$. Moreover,

$$(\varepsilon^{-\gamma}\phi_r^\varepsilon)^2 + (\varepsilon^{-\gamma}\phi_3^\varepsilon - 1)^2 = \left(\frac{s}{\varepsilon^\gamma} + \sqrt{2}\right)^2,$$

so under the choice $\delta \ge c_0\varepsilon^\gamma$ (with c_0 large enough) this quantity is ≥ 8 when $s = \delta/2$, and therefore $\boldsymbol{\psi} \equiv \mathbf{id}$ on $(\varepsilon^{-\gamma}\boldsymbol{\phi}_\varepsilon)^{-1}(\{s = \delta/2\})$. Consequently, $\boldsymbol{u}(\boldsymbol{x}) = \varepsilon^\gamma \boldsymbol{\psi}(\varepsilon^{-\gamma}\boldsymbol{\phi}_\varepsilon(\boldsymbol{x})) = \boldsymbol{\phi}_\varepsilon(\boldsymbol{x}) = \boldsymbol{b}_\delta(\boldsymbol{x})$ on $\{s = \delta/2\}$, so $\boldsymbol{b}_\delta$ matches continuously with $\boldsymbol{u}$ across the interface.

Transition layer in region d.

Within the neck d, the limit map $\boldsymbol{v}$ is singular on the axis: it collapses the vertical segment S to the origin, whereas $\boldsymbol{u}_\varepsilon$ "opens" the axis to form a cylindrical cavity of radius $\sim \varepsilon^\gamma$. A generic linear interpolation would introduce a gradient perturbation of order $\sim \varepsilon^\gamma/\delta$. However, we have also to control the determinant. The explicit construction is thus necessary.

Let $\boldsymbol{g}$ be the auxiliary map defined in (A.2) and (A.5). By the bi-Lipschitz property of the planar representative of $\boldsymbol{g}$, after possibly decreasing ε we can also ensure the separation of the image through $\boldsymbol{u}_\varepsilon$ of the level set $\operatorname{dist}(\boldsymbol{x}, U) = \delta/2$ and the image through $\boldsymbol{v}$ of the level set $\operatorname{dist}(\boldsymbol{x}, U) = \delta$. In particular, for ε small enough, $\delta/2 \ge 2\sqrt{2}\,\varepsilon^\gamma$, and for every $\boldsymbol{x} \in d \cap T_\delta$ we have $r = \operatorname{dist}(\boldsymbol{x}, U) \ge \delta/2$. We set

$$\boldsymbol{b}_\delta(\boldsymbol{x}) = w_r(\boldsymbol{x})\, \boldsymbol{e}_r(\theta) + w_3(\boldsymbol{x})\, \boldsymbol{e}_3,$$

where

$$\begin{cases} w_r(\boldsymbol{x}) := \chi_\delta(s)\omega_\varepsilon(z) + s\sin\varphi(z), \\ w_3(\boldsymbol{x}) := -s(r, x_3)\cos\varphi(z(r, x_3)), \end{cases} \tag{C.3}$$

with $z = z(r, x_3)$ the vertical coordinate in the intermediate configuration of Figure 4. The cut-off $\chi_\delta(s) = \frac{\delta - s}{\delta/2}$ reduces the "horizontal extrusion" $\omega_\varepsilon(z)\boldsymbol{e}_r$ from full magnitude at the level curve $\operatorname{dist}(\boldsymbol{x}, U) = \frac{\delta}{2}$ (where $\chi_\delta = 1$) to zero at the level curve $\operatorname{dist}(\boldsymbol{x}, U) = \delta$ (where $\chi_\delta = 0$). By the definition of $\boldsymbol{v}$ in (A.3) and the definition of $\boldsymbol{u}$ in (B.4), one has that $\boldsymbol{b}_\delta$ satisfies (C.1).

The idea is the following. In the image by $\boldsymbol{v}$ of the level curve at distance $s = \frac{\delta}{2}$, the zenithal angle φ (angle with respect to the downwards vertical semiaxis) goes from the ray $\varphi = \frac{\pi}{4}$ to the ray $\varphi = \frac{\pi}{2}$ (see Figure 1) for region d after the dipole deformation). This is reflected in the formula $\varphi(z) = \frac{\pi}{4}(1 + \frac{z}{3})$. The bottom-right point of the level curve $s = \frac{\delta}{2}$ in the reference configuration, namely, $(r = 1 + \frac{\delta}{2}, x_3 = 0)$, will be mapped to $z = 0$, ray $\varphi = \frac{\pi}{4}$, and radial coordinate $s = \frac{\delta}{2}$. Similarly, the top-right point of the level curve $s = \frac{\delta}{2}$ will be mapped to $z = 3$, ray $\varphi = \frac{\pi}{2}$, and radial coordinate $s = \frac{\delta}{2}$. These two points need to be joined by a circular arc of parameters $s = \frac{\delta}{2}$ and $\frac{\pi}{4} \le \varphi \le \frac{\pi}{2}$.

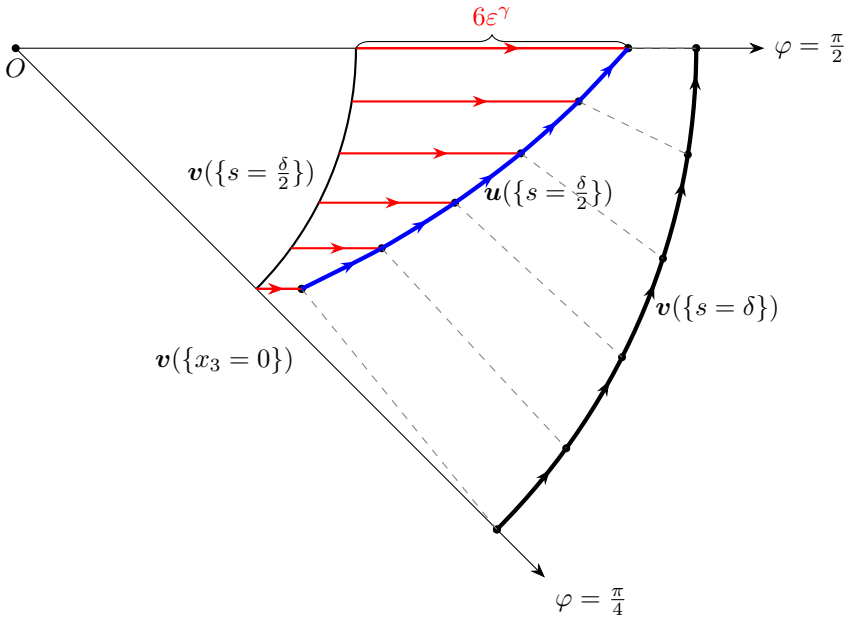


FIGURE 5. The red arrows illustrate the effect of the function $\omega_\varepsilon(z)$, which extrudes horizontally the image by $\boldsymbol{v}$ of the level curve $\{\boldsymbol{x} \in \Omega : s = \operatorname{dist}(\boldsymbol{x}, U) = \frac{\delta}{2}\}$. This gives rise to the blue curve, which is the image of the same level set by the approximating map $\boldsymbol{u}$. Our construction $\boldsymbol{b}_\delta$ interpolates linearly between that blue curve and the curve $\boldsymbol{v}(\{s = \delta\})$ on the right-end of the transition layer T_δ.

The image by $\boldsymbol{v}$ of the level curve at distance $s = \delta$ is also a circular arc, of parameters $s = \delta$ and $\frac{\pi}{4} \leq \varphi \leq \frac{\pi}{2}$. In our construction, on the right circular arc $\boldsymbol{b}_\delta$ must coincide with $\boldsymbol{v}$. On the left circular arc instead $\boldsymbol{b}_\delta$ is not the image curve $\frac{\delta}{2}$, since it must coincide with $\boldsymbol{u}$. Here $\boldsymbol{u}$ takes that curve and "extrudes it horizontally" by a distance $\omega_\varepsilon(z)$ that begins being ε^γ when $x_3 = 0$, $z = 0$, and ends up being $6\varepsilon^\gamma$ when $x_3 = 1$, $z = 3$ (see Figure 5). The idea, then, is to gradually reduce the magnitude of the horizontal extrusion, from $\omega_\varepsilon \sim \varepsilon^\gamma$ at distance $\frac{\delta}{2}$, to zero at distance δ. An observation to be made is that the branch $\hat{r}$ in the definition (B.5) of $\boldsymbol{u}_\varepsilon$ in region d does not affect us in the transition layer $\frac{\delta}{2} \leq s \leq \delta$. Indeed, $\hat{r} = r$ in the branch $r \geq \varepsilon^{2\gamma}$, and because of the assumption (C.2), in the region $s(r, x_3) \geq \delta/2$ we have $r \geq \delta/2 \geq \varepsilon^{2\gamma}$, for ε small enough.

Transition layer in region e.

Taking ε small enough, we can assume that T_δ does not intersect the region e'_ε. In e_ε, we have $\operatorname{dist}(\boldsymbol{x}, U) = \rho \cos\varphi$, where (ρ, θ, φ) are the spherical coordinates in this region. We set

$$\boldsymbol{b}_\delta(\boldsymbol{x}) = \big[(1 - \chi_\delta(\rho\cos\varphi))\, v_\rho(\rho,\varphi) + \chi_\delta(\rho\cos\varphi)\, u_\rho(\rho,\varphi)\big]\big(\sin\varphi\, \boldsymbol{e}_r(\theta) + \cos\varphi\, \boldsymbol{e}_3\big).$$

This matches $\boldsymbol{u}_\varepsilon$ when $\operatorname{dist}(\boldsymbol{x}, U) \leq \delta/2$ and $\boldsymbol{v}$ when $\operatorname{dist}(\boldsymbol{x}, U) \geq \delta$.

Transition layer in region f.

In this region the transition is straightforward, since $\boldsymbol{v}$ is regular and $\boldsymbol{u}_\varepsilon \to \boldsymbol{v}$ in C^1. Let

$$\chi(\boldsymbol{x}) := \frac{\delta - \operatorname{dist}(\boldsymbol{x}, U)}{\delta/2}.$$

For $\boldsymbol{x} \in T_\delta \cap f$, we set

$$\boldsymbol{b}_\delta(\boldsymbol{x}) := (1 - \chi(\boldsymbol{x}))\, \boldsymbol{v}(\boldsymbol{x}) + \chi(\boldsymbol{x})\, \boldsymbol{u}(\boldsymbol{x}).$$

Using the explicit formulas in the Appendices A and B, one can check that $|\boldsymbol{u} - \boldsymbol{v}| \leq c\,\varepsilon^\gamma$ and $|D\boldsymbol{u} - D\boldsymbol{v}| \leq c\,\varepsilon^\gamma$.

Step 2: uniform bound on the energy and orientation-preserving character.

We have to show that the energy contribution coming from the transition layer is bounded independently of δ.

Energy region b.

In $b \cap T_\delta$ we write

$$\boldsymbol{x} = \rho \sin\varphi\, \boldsymbol{e}_r(\theta) + \rho\cos\varphi\, \boldsymbol{e}_3, \qquad \frac{\pi}{2} \le \varphi \le \pi, \qquad s := \rho - 1 = \operatorname{dist}(\boldsymbol{x}, U) \in \Big[\frac{\delta}{2}, \delta\Big].$$

Recall that in b one has

$$\boldsymbol{b}_\delta(\boldsymbol{x}) = \Big(s + \chi_\delta(s)\sqrt{2}\,\varepsilon^\gamma\Big)\, \boldsymbol{d}(\varphi,\theta) + \chi_\delta(s)\,\varepsilon^\gamma\, \boldsymbol{e}_3, \qquad \boldsymbol{d}(\varphi,\theta) := \sin\Phi(\varphi)\, \boldsymbol{e}_r(\theta) + \cos\Phi(\varphi)\, \boldsymbol{e}_3,$$

with $\Phi(\varphi) := \frac{\varphi+\pi}{2}$. Set

$$r_\delta(s) := s + \chi_\delta(s)\sqrt{2}\,\varepsilon^\gamma, \qquad z_\delta(s) := \chi_\delta(s)\varepsilon^\gamma, \qquad \rho = 1 + s.$$

Since $\chi_\delta'(s) = -2/\delta$ on $[\delta/2, \delta]$ and $\delta \ge c_0\varepsilon^\gamma$ (see (C.2)), we have

$$|r_\delta'(s)| \le 1 + c\,\frac{\varepsilon^\gamma}{\delta} \le c, \qquad |z_\delta'(s)| \le c\,\frac{\varepsilon^\gamma}{\delta} \le c.$$

Moreover,

$$\partial_s \boldsymbol{b}_\delta = r_\delta'(s)\, \boldsymbol{d} + z_\delta'(s)\, \boldsymbol{e}_3, \qquad \partial_\varphi \boldsymbol{b}_\delta = \frac{1}{2}\, r_\delta(s)\big(\cos\Phi\, \boldsymbol{e}_r(\theta) - \sin\Phi\, \boldsymbol{e}_3\big), \qquad \partial_\theta \boldsymbol{b}_\delta = r_\delta(s)\sin\Phi\, \partial_\theta \boldsymbol{e}_r(\theta).$$

Using the metric factors of spherical coordinates and $\rho = 1 + s \simeq 1$ on T_δ, and using that, for $\frac{\pi}{4} \le \varphi \le \pi$,

$$\frac{\sin^2\Phi}{\sin^2\varphi} = \frac{\cos^2\left(\frac{\varphi}{2}\right)}{\sin^2\varphi} = \frac{1}{4\sin^2\left(\frac{\varphi}{2}\right)} \le 2, \tag{C.4}$$

we find that

$$|D\boldsymbol{b}_\delta(\boldsymbol{x})|^2 \le c\left(|\partial_s \boldsymbol{b}_\delta|^2 + \frac{1}{\rho^2}|\partial_\varphi \boldsymbol{b}_\delta|^2 + \frac{1}{\rho^2\sin^2\varphi}|\partial_\theta \boldsymbol{b}_\delta|^2\right) \le c\left(1 + \frac{\varepsilon^{2\gamma}}{\delta^2}\right),$$

and therefore

$$\int_{T_\delta \cap b} |D\boldsymbol{b}_\delta|^2\, \mathrm{d}\boldsymbol{x} \le c\left(\delta + \frac{\varepsilon^{2\gamma}}{\delta}\right) \le c.$$

For the determinant, in the coordinates (s, φ, θ) (see, e.g., [8, Appendix B.3]) one has

$$\begin{aligned}
\det D\boldsymbol{b}_\delta(\boldsymbol{x}) &= \frac{\det(\partial_s \boldsymbol{b}_\delta, \partial_\varphi \boldsymbol{b}_\delta, \partial_\theta \boldsymbol{b}_\delta)}{\rho^2 \sin\varphi} \\
&= \frac{1}{2}\,\frac{r_\delta(s)^2}{\rho^2}\,\frac{\sin\Phi(\varphi)}{\sin\varphi}\Big(r_\delta'(s) + z_\delta'(s)\cos\Phi(\varphi)\Big) \\
&= \frac{1}{2}\,\frac{r_\delta(s)^2}{\rho^2}\,\frac{\sin\Phi(\varphi)}{\sin\varphi}\Big(1 + \varepsilon^\gamma \chi_\delta'(s)\big(\sqrt{2} + \cos\Phi(\varphi)\big)\Big).
\end{aligned} \tag{C.5}$$

Since $\frac{\sin\Phi(\varphi)}{\sin\varphi} = \frac{1}{2\sin\left(\frac{\varphi}{2}\right)}$ (see (C.4)) is bounded above and below on $[\pi/2, \pi]$, choosing c_0 in (C.2) large enough yields

$$1 + \varepsilon^\gamma \chi_\delta'(s)\big(\sqrt{2} + \cos\Phi(\varphi)\big) \ge \frac{1}{2} \qquad \text{for } s \in [\delta/2, \delta].$$

We infer from (C.5) that $\det D\boldsymbol{b}_\delta(\boldsymbol{x}) \ge c\, s^2$ on $T_\delta \cap b$. Hence,

$$\int_{T_\delta \cap b} H(\det D\boldsymbol{b}_\delta)\, \mathrm{d}\boldsymbol{x} \le c \int_{\delta/2}^{\delta} s^{-2\alpha}\, \mathrm{d}s \le c,$$

independently of δ.

Energy region d.

Recall that in $d \cap T_\delta$ by (C.2) we have $r \geq \frac{\delta}{2} \geq 2\sqrt{2}\varepsilon^\gamma$. By the formula for the gradient in cylindrical-cylindrical coordinates (see, e.g., [8, Appendix B.2]),

$$D\boldsymbol{b}_\delta(\boldsymbol{x}) = \begin{pmatrix} \partial_r w_r & 0 & \partial_{x_3} w_r \\ 0 & \frac{w_r}{r} & 0 \\ \partial_r w_3 & 0 & \partial_{x_3} w_3 \end{pmatrix}.$$

In particular,

$$\det D\boldsymbol{b}_\delta = \frac{w_r}{r} \frac{\partial(w_r, w_3)}{\partial(r, x_3)}. \tag{C.6}$$

Let us first study the tangential stretch $\frac{w_r}{r}$. Thanks to (B.7), we have

$$\begin{aligned} w_r(\boldsymbol{x}) &= \frac{\delta - s(r,x_3)}{\delta/2} \omega_\varepsilon\big(z(r,x_3)\big) + s(r,x_3)\sin\varphi(z(r,x_3)) \\ \Rightarrow \quad & s\sin\varphi \leq w_r(\boldsymbol{x}) \leq \frac{\delta/2}{\delta/2} \cdot 6\varepsilon^\gamma + s\sin\varphi \\ \Rightarrow \quad & \frac{s\sin\varphi}{r} \leq \frac{w_r(\boldsymbol{x})}{r} \leq 2 + \frac{s}{r}\sin\varphi. \end{aligned} \tag{C.7}$$

The lower bound for $\frac{w_r(\boldsymbol{x})}{r}$ will be used to compare $\det D\boldsymbol{b}_\delta$ with $\det D\boldsymbol{v}$. By construction of $\boldsymbol{b}_\delta$, when we are close to the axis, we have $s = r$ (see (A.5)). In the rest of the region, s is still controlled by r; see Appendix A. Therefore, $\frac{w_r(\boldsymbol{x})}{r}$ is bounded from above by a constant, independently of ε.

Regarding the 2×2 minor in the expression for $\det D\boldsymbol{b}_\delta$, observe that

$$\frac{\partial(w_r, w_3)}{\partial(r, x_3)} = \frac{\partial(w_r, w_3)}{\partial(s, z)} \frac{\partial(s, z)}{\partial(r, x_3)}.$$

Note also that

$$\frac{\partial(s, z)}{\partial(r, x_3)} = \frac{\partial \boldsymbol{g}}{\partial r} \wedge \frac{\partial \boldsymbol{g}}{\partial x_3}$$

since $(r, x_3) \mapsto (s, z)$ is the 2D representation of the auxiliary transformation $\boldsymbol{g}(r\boldsymbol{e}_r + x_3\boldsymbol{e}_3) = s(r, x_3)\boldsymbol{e}_r + z(r, x_3)\boldsymbol{e}_3$. This 2D representation is bi-Lipschitz, as shown in Figure 4. Hence,

$$c^{-1} \frac{\partial(w_r, w_3)}{\partial(s, z)} \leq \frac{\partial(w_r, w_3)}{\partial(r, x_3)} \leq c \frac{\partial(w_r, w_3)}{\partial(s, z)}.$$

On the other hand,

$$\begin{aligned} \frac{\partial(w_r, w_3)}{\partial(s, z)} &= \begin{vmatrix} -\frac{2}{\delta}\omega_\varepsilon(z) + \sin\varphi & 2\frac{\delta - s}{\delta}\omega_\varepsilon'(z) + \frac{\pi}{12} s\cos\varphi \\ -\cos\varphi & \frac{\pi}{12} s\sin\varphi \end{vmatrix} \\ &= \tfrac{\pi}{12} s - \tfrac{2}{\delta}\omega_\varepsilon(z) \cdot \tfrac{\pi}{12} s\sin\varphi + \underbrace{\cos\varphi \cdot 2\tfrac{\delta - s}{\delta}\omega_\varepsilon'(z)}_{\geq 0} \qquad \text{(C.8)} \\ &\geq \tfrac{\pi}{12} s \left(1 - 2\frac{\omega_\varepsilon(z)}{\delta}\sin\varphi\right) \underset{\text{(B.7)}}{\geq} \tfrac{\pi}{12} s \left(1 - 2\frac{6\varepsilon^\gamma}{\delta}\sin\varphi\right) \underset{\text{(C.2)}}{\geq} c\, s. \qquad \text{(C.9)} \end{aligned}$$

Since $\frac{\pi}{4} \leq \varphi \leq \frac{\pi}{2}$, combining (C.6), (C.7), and (C.9) yields that

$$\det D\boldsymbol{b}_\delta(\boldsymbol{x}) \geq c \frac{s^2(r, x_3)\sin\varphi(z(r, x_3))}{r} \geq c \det D\boldsymbol{v}(\boldsymbol{x}) \geq c \frac{s^2(r, x_3)}{r}.$$

Similarly, from (B.8), (C.6), (C.7), and (C.8), we obtain the upper bound

$$\det D\boldsymbol{b}_\delta(\boldsymbol{x}) \leq c.$$

Therefore, $\int_{T_\delta \cap d} H(\det D\boldsymbol{b}_\delta) \le c$ independently of δ (compare with (A.6)). After a change of coordinates from (r, x_3) to (s, z), using (B.7) and (B.8), each term on $D\boldsymbol{b}_\delta$ other than the tangential stretch $\frac{w_r}{r}$ can be controlled.

Energy region e.

In this region the map $\boldsymbol{v}$ degenerates at the boundary $\varphi = \pi/2$. We use spherical coordinates. The radial component is given by $b_\rho = \chi_\delta u_\rho + (1-\chi_\delta)v_\rho$. Since the angular components coincide ($b_\varphi = v_\varphi = u_\varphi = \varphi$), the Jacobian[3] is

$$\det D\boldsymbol{b}_\delta = \frac{(b_\rho)^2}{\rho^2}\partial_\rho b_\rho.$$

We must check that $\partial_\rho b_\rho > 0$. Differentiating the interpolation gives

$$\partial_\rho b_\rho = \chi_\delta \partial_\rho u_\rho + (1-\chi_\delta)\partial_\rho v_\rho + \chi'_\delta(u_\rho - v_\rho)\partial_\rho \operatorname{dist}(\boldsymbol{x}, U).$$

In this region, $\operatorname{dist}(\boldsymbol{x}, U) = \rho\cos\varphi$, so that $\partial_\rho \operatorname{dist}(\boldsymbol{x}, U) = \cos\varphi$. Specifically, we have the following estimates:

(i) For the convex combination term: since $\partial_\rho u_\rho \ge \cos\varphi$ (see [8, p. 39, Eq. (3.33)]) and $\partial_\rho v_\rho = \cos\varphi$, we have

$$\chi_\delta \partial_\rho u_\rho + (1-\chi_\delta)\partial_\rho v_\rho \ge \cos\varphi.$$

(ii) For the perturbation term: we have $\chi'_\delta = -2/\delta$ and $|u_\rho - v_\rho| \le 7\varepsilon^\gamma$. Indeed, writing

$$u_\rho(\rho,\varphi) - v_\rho(\rho,\varphi) = \frac{1-\rho}{1-\varepsilon}(u_\rho(\varepsilon,\varphi) - \cos\varphi) + \frac{\rho-\varepsilon}{1-\varepsilon}\cdot 6\varepsilon^\gamma - \frac{\varepsilon(1-\rho)}{1-\varepsilon}\cos\varphi$$

and considering that $\cos\varphi \le u_\rho(\varepsilon,\varphi) \le \cos\varphi + 6\varepsilon^\gamma$ (see [8, Eq. (3.10)]), it is possible to see that

$$u_\rho(\rho,\varphi) - v_\rho(\rho,\varphi) \ge \frac{-\varepsilon(1-\rho)}{1-\varepsilon}\cos\varphi \ge -2\varepsilon\cos\varphi.$$

On the other hand,

$$u_\rho - v_\rho \le \frac{1-\rho}{1-\varepsilon}\cdot 6\varepsilon^\gamma + \frac{\rho-\varepsilon}{1-\varepsilon}\cdot 6\varepsilon^\gamma + \frac{1}{1-\varepsilon}\cdot \varepsilon^\gamma \cdot 1 \le 7\varepsilon^\gamma.$$

Consequently,

$$\chi'_\delta(u_\rho - v_\rho)\partial_\rho \operatorname{dist}(\boldsymbol{x}, U) \ge -\frac{2}{\delta}(7\varepsilon^\gamma)\cos\varphi = -\frac{14\varepsilon^\gamma}{\delta}\cos\varphi.$$

Combining these, we factor out the term $\cos\varphi$:

$$\partial_\rho b_\rho \ge \cos\varphi\left(1 - \frac{14\varepsilon^\gamma}{\delta}\right).$$

Since $\cos\varphi > 0$ for $\varphi \in [0, \pi/2)$, we have that $\partial_\rho b_\rho$ is comparable to $\partial_\rho v_\rho$ up to a strictly positive multiplicative constant, provided we choose $c_0 > 14$ in (C.2). In addition, the lower bound on $u_\rho - v_\rho$ established above gives

$$b_\rho = \chi_\delta u_\rho + (1-\chi_\delta)v_\rho = v_\rho + \chi_\delta(u_\rho - v_\rho) \ge v_\rho - 2\varepsilon\cos\varphi = (1+\rho-2\varepsilon)\cos\varphi.$$

Since $\rho \le 1$ and ε is small (in particular $\varepsilon < 1/4$), we have $1+\rho-2\varepsilon \ge \frac{1}{2}(1+\rho)$, and therefore $b_\rho^2 \ge \frac{1}{4}(1+\rho)^2\cos^2\varphi = \frac{1}{4}\,v_\rho^2$. Hence

$$\det D\boldsymbol{b}_\delta = \frac{b_\rho^2}{\rho^2}\,\partial_\rho b_\rho \ge \frac{1}{4}\,\frac{v_\rho^2}{\rho^2}\cdot c\,\partial_\rho v_\rho = c\,\det D\boldsymbol{v} \qquad \text{on } T_\delta \cap e.$$

[3] See, e.g., [8, Appendix B.3]

We now bound the H term. Since $\det D\boldsymbol{b}_\delta \geq c \det D\boldsymbol{v}$ on $T_\delta \cap e$ and H is decreasing near 0, we have $H(\det D\boldsymbol{b}_\delta) \leq H(c \det D\boldsymbol{v})$. Therefore, from the integrability of $H(\det D\boldsymbol{v})$ established in Appendix A, $\int_{T_\delta \cap e} H(\det D\boldsymbol{b}_\delta)\,\mathrm{d}\boldsymbol{x} \leq c$ independently of δ.

Energy region f.

In $f \cap T_\delta$ we use the convex interpolation

$$\boldsymbol{b}_\delta = (1-\chi)\boldsymbol{v} + \chi \boldsymbol{u}, \quad \chi(\boldsymbol{x}) := \frac{\delta - \operatorname{dist}(\boldsymbol{x}, U)}{\delta/2} \in [0,1], \quad |\nabla \chi| = \frac{2}{\delta}.$$

Since

$$D\boldsymbol{b}_\delta = D\boldsymbol{v} + \chi\, D(\boldsymbol{u}-\boldsymbol{v}) + (\boldsymbol{u}-\boldsymbol{v}) \otimes \nabla \chi,$$

and, by the explicit formulas in Appendices A and B, $|\boldsymbol{u}-\boldsymbol{v}| \leq c\,\varepsilon^\gamma$ and $|D\boldsymbol{u} - D\boldsymbol{v}| \leq c\,\varepsilon^\gamma$ in this region, we get

$$|D\boldsymbol{b}_\delta| \leq |D\boldsymbol{v}| + 6\varepsilon^\gamma\Big(\sqrt{2} + \frac{2}{\delta}\Big).$$

Since the dipole $\boldsymbol{v}$ is C^1 in region f, it follows that

$$\int_{T_\delta \cap f} |D\boldsymbol{b}_\delta|^2\, d\boldsymbol{x} \leq c.$$

For the determinant, note that

$$\boldsymbol{b}_\delta = b_\rho\big(\boldsymbol{x}(\rho,\varphi)\big)\,(\sin\varphi\, \boldsymbol{e}_r + \cos\varphi\, \boldsymbol{e}_3), \qquad b_\rho = v_\rho(\rho,\varphi) + \chi\big(\boldsymbol{x}(\rho,\varphi)\big)\cdot 6\varepsilon^\gamma.$$

Hence $b_\rho \geq v_\rho(\rho,\varphi)$, and

$$\partial_\rho b_\rho = \partial_\rho v_\rho + 6\varepsilon^\gamma\, \nabla\chi \cdot \partial_\rho \boldsymbol{x} \geq \partial_\rho v_\rho - 6\varepsilon^\gamma\, |\nabla\chi| = 1 - \frac{12\varepsilon^\gamma}{\delta}.$$

Therefore, if $c_0 > 12$ in (C.2),

$$\det D\boldsymbol{b}_\delta = \frac{b_\rho^2}{\rho^2}\,\partial_\rho b_\rho \geq \frac{v_\rho^2}{\rho^2}\Big(1 - \frac{12\varepsilon^\gamma}{\delta}\Big) \geq c \det D\boldsymbol{v} \quad \text{on } T_\delta \cap f. \tag{C.10}$$

For the H term, since H is decreasing near zero, (C.10) gives $H(\det D\boldsymbol{b}_\delta) \leq H(c \det D\boldsymbol{v})$ on $T_\delta \cap f$. In particular, $\int_{T_\delta \cap f} H(\det D\boldsymbol{b}_\delta)\, d\boldsymbol{x} \leq c$ independently of δ.

Collecting the constraints on the constant c_0 in (C.2), we need:

- in region b, positivity of the Jacobian: $c_0 > 4\sqrt{2}$;
- in region d, positivity of the Jacobian: $c_0 > 12$;
- in region e, positivity of $\partial_\rho b_\rho$: $c_0 > 14$;
- in region f, positivity of $\partial_\rho b_\rho$: $c_0 > 12$;
- in region b, injectivity of the planar profile: $c_0 > 2\sqrt{2}$;
- matching with $\boldsymbol{\psi} \equiv \mathbf{id}$ at $s = \delta/2$: $c_0 \geq 4$.

Thus the binding condition is $c_0 > 14$.

Step 3: bi-Lipschitz properties.

We prove that the map $\boldsymbol{b}_\delta$ constructed in Step 1 is bi-Lipschitz on $B(\mathbf{0},4)$. Recall that $\boldsymbol{b}_\delta = \boldsymbol{u}$ on $U_{\delta/2}$ and $\boldsymbol{b}_\delta = \boldsymbol{v}$ on $B(\mathbf{0},4) \setminus U_\delta$. Moreover, $\boldsymbol{b}_\delta$ is continuous across all interfaces by construction.

(i) $\boldsymbol{b}_\delta$ is Lipschitz. The domain $B(\mathbf{0},4)$ is partitioned into the following subdomains: the core $U_{\delta/2}$, the exterior $B(\mathbf{0},4) \setminus U_\delta$, and the four pieces $T_\delta \cap b$, $T_\delta \cap d$, $T_\delta \cap e$, $T_\delta \cap f$. On each of these pieces, $\boldsymbol{b}_\delta$ is piecewise C^1 and the estimates of Step 2 (together with the explicit formulas in Step 1) give the bound

$$\|D\boldsymbol{b}_\delta\|_{L^\infty(B(\mathbf{0},4))} \leq C(\delta) < \infty. \tag{C.11}$$

Since the traces match on the interfaces, no jump part appears in the distributional gradient; by (C.11), $\boldsymbol{b}_\delta$ is Lipschitz.

(ii) Pointwise bound on the inverse matrix. We apply the elementary estimate

$$|\boldsymbol{A}^{-1}| \le \frac{c\,|\boldsymbol{A}|^2}{\det \boldsymbol{A}}, \qquad \text{for any } \boldsymbol{A} \in \mathbb{R}^{3\times 3} \text{ with } \det \boldsymbol{A} > 0 \tag{C.12}$$

to $\boldsymbol{A} = D\boldsymbol{b}_\delta(\boldsymbol{x})$. By construction, $\boldsymbol{b}_\delta$ coincides with $\boldsymbol{u} = \boldsymbol{u}_\varepsilon$ on $U_{\delta/2}$ and with $\boldsymbol{v}$ on $B(\mathbf{0},4)\setminus U_\delta$. Since $\boldsymbol{u}$ is bi-Lipschitz on $B(\mathbf{0},4)$ (Appendix B, property (i)) and $\boldsymbol{v}$ is bi-Lipschitz on $B(\mathbf{0},4)\setminus U_\delta$ (where it is regular), $\det D\boldsymbol{b}_\delta$ is bounded away from zero on each of these two pieces, with constants that may depend on δ (and hence on ε). It remains to check its positivity in the transition layer T_δ. There, the determinant estimates established in Step 2 give:

- In regions b, d, and f: $\det D\boldsymbol{b}_\delta \ge c\,s^2/r$. Since $s \ge \delta/2$ and $r \le 3$ on T_δ, we obtain $\det D\boldsymbol{b}_\delta \ge c\,\delta^2$.
- In region e: $\det D\boldsymbol{b}_\delta \ge c \det D\boldsymbol{v} = c\,(1+\rho)^2\rho^{-2}\cos^3\varphi$. On $T_\delta \cap e$ one has $\operatorname{dist}(\boldsymbol{x}, U) = \rho\cos\varphi \ge \delta/2$ and $\rho \le 1$, so $\cos\varphi \ge \delta/(2\rho) \ge \delta/2$ and $(1+\rho)^2/\rho^2 \ge 1$. Hence $\det D\boldsymbol{b}_\delta \ge c\,\delta^3$.

Combining these bounds with the positivity on $U_{\delta/2}$ and $B(\mathbf{0},4)\setminus U_\delta$, we conclude that

$$m(\delta) := \operatorname{essinf}_{B(\mathbf{0},4)} \det D\boldsymbol{b}_\delta \;>\; 0. \tag{C.13}$$

The value of $m(\delta)$ depends on δ through both the transition-layer estimates and the bi-Lipschitz constants of $\boldsymbol{u}_{\varepsilon(\delta)}$. Combining (C.11), (C.12) and (C.13) yields

$$\|(D\boldsymbol{b}_\delta)^{-1}\|_{L^\infty(B(\mathbf{0},4))} \le \frac{c\,\|D\boldsymbol{b}_\delta\|_{L^\infty}^2}{m(\delta)} \;=\; C(\delta) < \infty. \tag{C.14}$$

(iii) Injectivity and Lipschitz continuity of the inverse. We next argue that $\boldsymbol{b}_\delta$ is a homeomorphism. On $U_{\delta/2}$ and on $B(\mathbf{0},4)\setminus U_\delta$ this follows from the fact that $\boldsymbol{u}$ and $\boldsymbol{v}$ are homeomorphisms. In the transition layer T_δ we treat each region separately:

- In region b, the map $\boldsymbol{b}_\delta$ has the form

  $$\boldsymbol{b}_\delta(\rho,\varphi,\theta) = r_\delta(\rho-1)\,\boldsymbol{d}(\varphi,\theta) + z_\delta(\rho-1)\,\boldsymbol{e}_3,$$

  where

  $$r_\delta(s) := s + \chi_\delta(s)\sqrt{2}\,\varepsilon^\gamma, \qquad z_\delta(s) := \chi_\delta(s)\varepsilon^\gamma.$$

  The angular variables (φ,θ) are preserved, and the planar map $s \mapsto (r_\delta(s), z_\delta(s))$ is injective on $[\delta/2,\delta]$ since

  $$r_\delta'(s) = 1 - \frac{2\sqrt{2}\,\varepsilon^\gamma}{\delta} > 0$$

  whenever $c_0 > 2\sqrt{2}$.
- In region d, the planar representative in (r, x_3) is the composition of the bi-Lipschitz map $(r,x_3) \mapsto (s,z)$ (planar representative of $\boldsymbol{g}$) with the explicit map $(s,z) \mapsto (w_r, w_3)$ given by (C.3). The determinant lower bound in $d \cap T_\delta$ (see Step 2) prevents degeneracy, and the choice (C.2) (with c_0 large) ensures that the images of the two boundary components $\{s = \delta/2\}$ and $\{s = \delta\}$ are separated (see Figure 5), hence injectivity holds.
- In region e, the angular variables (φ,θ) are again preserved, and the radial profile $b_\rho(\rho,\varphi)$ is strictly increasing in ρ because

  $$\partial_\rho b_\rho \ge \cos\varphi\left(1 - \frac{14\varepsilon^\gamma}{\delta}\right) > 0$$

  by Step 2. Hence, for every φ, the map $\rho \mapsto b_\rho(\rho,\varphi)$ is injective.

- In region f, $\boldsymbol{v}$ is regular and $\boldsymbol{u}_\varepsilon \to \boldsymbol{v}$ in C^1; thus, for ε sufficiently small, the convex interpolation defining $\boldsymbol{b}_\delta$ remains injective (this is a standard stability property of bi-Lipschitz maps under C^1 perturbations).

Since $\boldsymbol{b}_\delta$ is continuous and injective on the compact set $\overline{B(\mathbf{0},4)}$, it is a homeomorphism onto its image.

Finally, because $\boldsymbol{b}_\delta$ is piecewise C^1 and $\det D\boldsymbol{b}_\delta > 0$, the restriction of $\boldsymbol{b}_\delta$ to each piece is a C^1 diffeomorphism. Hence the inverse is C^1 on each corresponding image piece and satisfies

$$D(\boldsymbol{b}_\delta^{-1}) = (D\boldsymbol{b}_\delta)^{-1} \circ \boldsymbol{b}_\delta^{-1}$$

there. Using (C.14), we obtain a Lipschitz bound for $\boldsymbol{b}_\delta^{-1}$ on each image piece. Since the image pieces cover $\boldsymbol{b}_\delta(B(\mathbf{0},4))$ and intersect only along their boundaries (where the traces match), the inverse $\boldsymbol{b}_\delta^{-1}$ is globally Lipschitz on $\boldsymbol{b}_\delta(B(\mathbf{0},4))$.

Therefore $\boldsymbol{b}_\delta$ is bi-Lipschitz. □

Acknowledgements. D. Henao was supported by FONDECYT grant N. 1231401 and by Center for Mathematical Modeling, FB210005, Basal ANID Chile.

C. Mora-Corral has been supported by the Spanish Agencia Estatal de Investigación through projects PID2024-158664NB-C2, PCI2024-155023-2 and CEX-2023-001347-S.

The research of R. Rodiac has been supported by the French government, through the **UCA**^{JEDI} Investments in the Future project managed by the National Research Agency (ANR) with the reference number ANR-15-IDEX-01.

The hospitality of Vera & Asociados Ltda. during the preparation of the manuscript is gratefully acknowledged.

References

[1] S. Almi, S. Krömer, and A. Molchanova. A new example for the Lavrentiev phenomenon in nonlinear elasticity. *Z. Angew. Math. Phys.*, 75(1):21, 2024. Id/No 2.

[2] J. M. Ball. Discontinuous equilibrium solutions and cavitation in nonlinear elasticity. *Philos. Trans. Roy. Soc. London Ser. A*, 306(1496):557–611, 1982.

[3] J. M. Ball. Some open problems in elasticity. In *Geometry, mechanics, and dynamics*, pages 3–59. Springer, New York, 2002.

[4] J. M. Ball and V. J. Mizel. One-dimensional variational problems whose minimizers do not satisfy the Euler-Lagrange equation. *Arch. Ration. Mech. Anal.*, 90:325–388, 1985.

[5] J. M. Ball and F. Murat. $W^{1,p}$-quasiconvexity and variational problems for multiple integrals. *J. Funct. Anal.*, 58(3):225–253, 1984.

[6] M. Barchiesi, D. Henao, and C. Mora-Corral. Local invertibility in Sobolev spaces with applications to nematic elastomers and magnetoelasticity. *Arch. Rational Mech. Anal.*, 224(2):743–816, 2017.

[7] M. Barchiesi, D. Henao, C. Mora-Corral, and R. Rodiac. Harmonic dipoles and the relaxation of the neo-Hookean energy in 3D elasticity. *Arch. Ration. Mech. Anal.*, 247(4):Paper No. 70, 46, 2023.

[8] M. Barchiesi, D. Henao, C. Mora-Corral, and R. Rodiac. On the lack of compactness in the axisymmetric neo-Hookean model. *Forum of Mathematics, Sigma*, 12:e26, 2024.

[9] M. Barchiesi, D. Henao, C. Mora-Corral, and R. Rodiac. A relaxation approach to the minimization of the neo-Hookean energy in 3D. *SIAM J. Math. Anal.*, 56(6):7830–7845, 2024.

[10] O. Bouchala, S. Hencl, and Z. Zhu. Weak limit of $W^{1,2}$ homeomorphisms in $\mathbb{R}^3$ can have any degree. *Ann. Fenn. Math.*, 49(2):547–560, 2024.

[11] D. Campbell, A. Doležalová, and S. Hencl. Mission $p < n-1$: possible – nonlinear elasticity beyond conventional limits. Preprint, arXiv:2506.07543, 2025.

[12] P. G. Ciarlet and J. Nečas. Injectivity and self-contact in nonlinear elasticity. *Arch. Rational Mech. Anal.*, 97(3):171–188, 1987.

[13] S. Conti and C. De Lellis. Some remarks on the theory of elasticity for compressible Neohookean materials. *Ann. Sc. Norm. Super. Pisa Cl. Sci. (5)*, 2(3):521–549, 2003.

[14] A. Doležalová, S. Hencl, and J. Malý. Weak limit of homeomorphisms in $W^{1,n-1}$ and (INV) condition. *Arch. Ration. Mech. Anal.*, 247(5):54, 2023. Id/No 80.

[15] A. Doležalová, S. Hencl, and A. Molchanova. Weak limit of homeomorphisms in $W^{1,n-1}$: invertibility and lower semicontinuity of energy. *ESAIM, Control Optim. Calc. Var.*, 30:32, 2024. Id/No 37.

[16] L. C. Evans and R. F. Gariepy. *Measure theory and fine properties of functions*. Textb. Math. Boca Raton, FL: CRC Press, revised ed. edition, 2015.
[17] H. Federer. *Geometric measure theory*. Springer, New York, 1969.
[18] M. Foss. Examples of the Lavrentiev phenomenon with continuous Sobolev exponent dependence. *J. Convex Anal.*, 10(2):445–464, 2003.
[19] M. Foss, W. Hrusa, and V. J. Mizel. The Lavrentiev phenomenon in nonlinear elasticity. *J. Elasticity*, 72(1-3):173–181, 2003.
[20] M. Foss, W. J. Hrusa, and V. J. Mizel. The Lavrentiev gap phenomenon in nonlinear elasticity. *Arch. Ration. Mech. Anal.*, 167(4):337–365, 2003.
[21] M. Giaquinta, G. Modica, and J. Souček. *Cartesian currents in the calculus of variations. I.* Springer-Verlag, Berlin, 1998.
[22] M. Giaquinta, G. Modica, and J. Souček. *Cartesian currents in the calculus of variations. II.* Springer-Verlag, Berlin, 1998.
[23] R. Hardt and F.-H. Lin. A remark on H^1 mappings. *Manuscripta Math.*, 56(1):1–10, 1986.
[24] R. Hardt, F.-H. Lin, and C.-C. Poon. Axially symmetric harmonic maps minimizing a relaxed energy. *Comm. Pure Appl. Math.*, 45(4):417–459, 1992.
[25] D. Henao and C. Mora-Corral. Invertibility and weak continuity of the determinant for the modelling of cavitation and fracture in nonlinear elasticity. *Arch. Rational Mech. Anal*, 197:619–655, 2010.
[26] D. Henao and C. Mora-Corral. Fracture surfaces and the regularity of inverses for BV deformations. *Arch. Rational Mech. Anal.*, 201(2):575–629, 2011.
[27] D. Henao and C. Mora-Corral. Lusin's condition and the distributional determinant for deformations with finite energy. *Adv. Calc. Var.*, 5(4):355–409, 2012.
[28] P. Kalayanamit. Sobolev regularity of the inverse for minimizers of the neo-Hookean energy satisfying condition INV. *Proceedings of the Royal Society of Edinburgh: Section A Mathematics*, page 1–21, 2025.
[29] K. Mazowiecka and P. Strzelecki. The Lavrentiev gap phenomenon for harmonic maps into spheres holds on a dense set of zero degree boundary data. *Adv. Calc. Var.*, 10(3):303–314, 2017.
[30] S. Müller and S. J. Spector. An existence theory for nonlinear elasticity that allows for cavitation. *Arch. Rational Mech. Anal.*, 131(1):1–66, 1995.

(Marco Barchiesi) Dipartimento di Matematica, Informatica e Geoscienze, Università degli Studi di Trieste, Via Weiss 2 - 34128 Trieste, Italy.
Email address: barchies@gmail.com

(Duvan Henao) Instituto de Ciencias de la Ingeniería, Universidad de O'Higgins. Rancagua, Chile
Email address: duvan.henao@uoh.cl

(Carlos Mora-Corral) Departamento de Matemáticas, Universidad Autónoma de Madrid, 28049 Madrid, Spain and Instituto de Ciencias Matemáticas, CSIC-UAM-UC3M-UCM, 28049 Madrid, Spain.
Email address: carlos.mora@uam.es

(Rémy Rodiac) Laboratoire J.A. Dieudonné, Université Côte d'Azur, CNRS UNMR 7351,06108, Nice, France.
Email address: remy.rodiac@univcotedazur.fr